Spring 5-4-2019

The Role of Neutrophils in Pancreatic Cancer

Edson DeOliveira
University of Nebraska Medical Center

The Role of Neutrophils in Pancreatic Cancer

by

Edson DeOliveira

A THESIS

Presented to the Faculty of
the University of Nebraska Graduate College in
Partial Fulfillment of the Requirements for the
Degree of Master of Science

Genetics, Cell Biology, and Anatomy
Graduate Program

Under the Supervision of Professor Leah Cook

University of Nebraska Medical Center

Omaha, Nebraska

April,
2019

Advisory Committee:

Leah Cook, Ph.D.

Karen Gould, Ph.D.

Rakesh Singh, Ph.D.

Joyce Solheim, Ph.D.

Acknowledgments

I would like to thank my thesis committee, Dr. Cook, Dr. Gould, Dr. Singh, and Dr. Solheim for their guidance. Additionally, thank you to Diane Costanzo and Tyler Keeley for their support and expertise throughout this project. I would also like to thank Megan Brown for helping arrange meeting locations and the Pathology and Microbiology department for use of their facilities for my project. Lastly, I am grateful for everyone else who has supported me towards the completion of this project.

The Role Of Neutrophils In Pancreatic Cancer

Edson DeOliveira, M.S.
University of Nebraska Medical Center, 2019

Advisor: Leah Cook, PhD

Pancreatic cancer is the fourth leading cause of cancer-related mortalities and the American Cancer Society estimates that 56,770 people will die of the disease in 2019. Known mutations include Kras oncogene, cyclin-dependent kinase inhibitor 2A (CDKN2A), TP53 and SMAD4. The current standard-of-care includes chemotherapies, but despite such approaches advanced staged patients have a relative 5-year survival rate of 8.5% overall. Immune cells such as neutrophils are believed to play a dual role in tumor eradication or tumor promotion. The aim of this study was to understand the effect of primary and metastatic pancreatic cancers on neutrophil NET formation and how NETs influence cancer cell survival. Results showed increases in neutrophil viability and NET formation in both nonmetastatic and metastatic condition medias. In patient samples, colocalization staining for myeloperoxidase (MPO) and citrullinated H3 (CitH3), differences in neutrophil infiltration and NET formation across tissue sample sites were observed but found to be not significant. However, in-vitro cocultures of neutrophil-cancer indicated that NET mediated reduction in cancer cell number was greater than 40% in nonmetastatic cell lines when compared to metastatic, and this alleviated by addition of a NET inhibitor GSK484. In an orthotopic mouse model, injection of luciferase expressing primary tumor (MiaPaca-2) cells, anti-Ly6G antibody neutrophil depleted groups showed hindered increases in tumor size suggest neutrophils may have had protumor role. However, final tumor size increase in neutrophil depleted groups was significant when compared to control, suggesting that additional cell populations may have modulated a tumor supporting function in place of neutrophils.

List of Figures

Figure 1 2

Histological features of PanINs and PDAC. A. Normal histology with (D) indicating a duct; (I) indicating a pancreatic islet cell; (A) showing pancreatic acinar cells. Staging dependent on extent of atypical cytological structure. PanIN1 A,B, arrows illustrate elongation of ductal cells with minimal nuclear deformation highlighting precancerous condition. PanIN 2 arrows indicate loss of mucous epithelium, nuclear crowding, and mitotic figures. PanIN3 corresponds to pseudopapillary formation and carcinoma, high nuclear pleomorphism, and intraluminal debris.

Figure 2 4

Immunohistochemical analysis comparing collagen deposition versus stellate cell activity around cancer structures. Immunohistochemistry performed using an anti-SMA antibody (brown) to detect activated PSCs and aniline (blue) to stain collagen fibers (B and D). (A and C) Density of activated PSCs increased around cancerous (unstained) structures. (A and B) Areas of activated PSCs colocalized with collagen deposition. (C and D).

Figure 3 5

Hematopoietic development of neutrophils. The development of neutrophils from long term hematopoietic stem cells (LT-HSC) to ST-HSC, MPP, LMPP, GMP, Myeloblast, promyelocyte, myelocyte, metamyelocyte, band cell and mature neutrophils. Cell surface molecule expression levels fluctuate dependent on stage of development. Ligands to CXCR4 retain neutrophils, while, CXCR2 recruit mature neutrophils out into circulation.

Figure 4 7

Net Formation. Illustration of active neutrophil undergoing NETosis. Expelled decondensed DNA contains various proteases including neutrophil elastase (NE, myeloperoxidase (MPO), cathepsin G, and histones in response to microbial pathogens.

Figure 5 7

Molecular pathways involved in NETosis. Microbial interaction with pathogen recognition receptors or phorbol-myristeacetate (PMA) induced elevation of intracellular calcium on neutrophils subsequently activates protein kinase C (PKC) and NAPDH oxidase. Reactive oxygen species (ROS) generated by NADPH oxidase leads to downstream signaling mediated by Akt, extracellular signal regulated kinsase (ERK1/2) and p38 mitogen-activated protein kinase (MAPK). Chromatin decondensation requires relocation of myeloperoxidase (MPO) and neutrophil elastase (NE) into the nucleus and histone citrullination (citH3), mediated by peptidylarginine deiminase 4 (PAD4). Activated platelets in response to lipopolysaccharide (LPS) or agonists such as thrombin can stimulate neutrophils to produced NETs via soluble or cell-mediated interactions

Figure 6 11

Potential role of monocyte and neutrophil associated myeloid suppressor cells (MDSCs) in the regulation of tumor development and progression. Tumor development is associated with the expansion of cells with acquired immunosuppressive activity (MDSCs). These cells also promote tumor cell invasion and angiogenesis and neutralize tumor cell senescence.

Figure 7 13

Activated Platelet Neutrophil NETosis interaction. In humans (left), platelet activation induces thromboxane A2 (TXA2) formation. This activates release of high mobility group box 1 (HMGB1), platelet factor 4 (PF4), and von Willebrand factor (vWF). CD18 on neutrophils is bound to both vWF, bound to its platelet receptor, and glycoprotein (GP)lb. In mice (right), platelet induced NET formation is carried out through G-protein coupled receptors (GPCR) via HMGB1, PF4, as well as thromboxane 2 (TXA2) PF4 and RANTES. Additionally, binding between P-selectin expressed on platelets and PSGL-1 receptors on neutrophils, is also required for the release of NETs.

Figure 8 22

Mouse bone marrow and human peripheral blood derived neutrophil survival sssay. (A) Serum free RPMI (control) was compared to MiaPaca (primary tumor cell line) and Capan (liver metastatic cell line) conditioned medias. (B) Serum free RPMI (control) was compared to Miapaca, Capan, S2013 (liver metastasis), and S2007 (lymph node) conditioned medias on neutrophil survival. Time points of 0, 18, 24, 36 hours were used for both experiments.

Figure 9 A-D 24

Induction of NET formation by cancer cell conditioned medias. Neutrophils were isolated and cultured for 4 hours in RMPI+2%BSA, RPMI+2%BSA+PMA, Miapaca-2, Capan-1, AsPC1, and S2013 conditioned media all with 2% BSA. (A,B) Mouse neutrophil incubated in pancan conditioned medias. (C,D) Human neutrophils incubated in pancan conditioned medias.

Figure 10A 26

Representative data illustrating neutrophil infiltration and NETosis colocalization between 6 patients matched samples of pancreas, liver, lungs. Sites of primary tumor and metastasis were patient matched and neutrophils and NETs were quantified via hand counting on Image J software.

Figure 10B 27

Representative immunofluorescence images of samples from untreated and chemotherapy treated pancreatic cancer patients with primary tumor, liver and lung metastasis. Cells were fixed, permeabilized and stained for myeloperoxidase (MPO, orange) citrullinated histone H3 (green), and DAPI (blue). NETs were identified by co-localization of (MPO+CitH3).

Figure 11 28

Coculture of Mouse Neutrophils with Pancreatic Cell Lines. Comparison between primary pancreatic lines (MiaPaca, and AsPC1) and metastatic (S2013 and Capan) in direct coculture with mouse neutrophils. Experimental conditions evaluated cancer cell only, cancer cell + neutrophil,

cancer+neutrophil+GSK484 inhibitor, and cancer+GSK484 all ran in triplicate. Percent reduction is the fold change in cell number due to neutrophil killing of cancer cells. Percent reduction with GSK484 is the change in inhibition of cell killing by prevention of histone citrullination and the inability to produce NETs.

Figure 12 29

Growth curve comparing MiaPaca-2 with MiaPaca-2 luciferase expressing nonmetastatic cell lines. Cell counts correspond to time course of 24, 48, and 72 hours.

Figure 13 30

In vivo data from mouse study for injection of the Miapaca-Luc cells. (A) Bioluminescence reading of Miapaca luciferase expressing cells. Over course of 33 days anti-Ly6G(1A8) neutrophil depleted mice showed increase in cancer growth. (B) Ultrasound quantification of tumor volume changes in isotype control versus increased change in neutrophil depleted anti-Ly6G mice. (C) Representative ultrasound imaging of isotype control and Ly6G neutrophil depleted mice groups.

Table of Contents

Acknowledgements I

Abstract II

List of Figures III

Chapter 1: Introduction 1

Chapter 2: Methods 18

Chapter 3: Results 24

Chapter 4: Discussion 34

Bibliography 39

Chapter 1: Introduction

Pancreatic Cancer Clinical Implications

The American Cancer Society estimates that 56,770 people (29,940 men and 26,830 women) will be diagnosed with pancreatic cancer and 45,750 will succumb to the disease in 2019. The causes of pancreatic cancer are still insufficiently known, although certain risk factors, common in other cancers but applicable to pancreatic care, including genetics, diabetes, diet, obesity, lack of exercise, and smoking, have been identified as predisposing individuals to higher rates of incidence (Ilic, 2016). Additionally, the risk of developing pancreatic cancer increases with age with over 80% of pancreatic cancer cases developing between the ages of 60 and 80 years (Yadav, 2013). With limited early detection methods, diagnosis often occurs at a late stage of the disease with fewer than 20% of patients being eligible for surgical resection (Martisian, 2019).

The current standard-of-care therapy includes chemotherapies, such as gemcitabine and folfirinox with or without radiation, with immunotherapies such as monoclonal antibodies (mAb) and antibody drug conjugates currently under development (Chiorean, 2015). Given its late diagnosis, individuals with advanced pancreatic cancer have a very poor prognosis, with a relative 5-year survival rate of 8.5% overall (Sohal, 2017). Current detection strategies for curable precursor lesions involve exploration of pancreatic cancer stromal markers. The benign tumor to malignant cancer transformation commonly seen in various cancers follows the sequence of initiation, clonal expansion, and metastasis to foreign microenvironments (Makohon-Moore, 2016). This sequence of events has led to screening for silent pancreatic neoplasias in individuals with family histories of pancreatic cancer (Kong, 2012). Of importance were screenings for potential tumor promoting factors expressed by molecules within the stromal environment. Screening for molecular factors secreted by stromal cells, in conjunction with current knowledge

in histological classification, could better validate early identification in pancreatic intrepithelial neoplasias (PanIN) to more severe pancreatic ductal adenocarcinoma (PDAC) progression models. Highlighted structural changes can be seen in various stages of pancreatic cancer with an increasing number of gene alterations positively correlating with higher grade PanINs (Fig. 1).

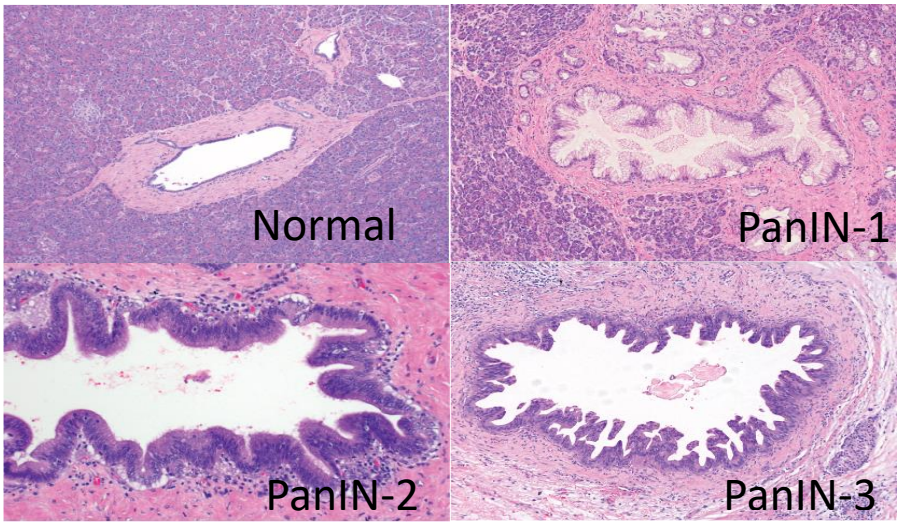

Figure 1|Histological features of PanINs and PDAC. A. Normal histology with (D) indicating a duct; (I) indicating a pancreatic islet cell; (A) showing pancreatic acinar cells. Staging dependent on extent of atypical cytological structure. PanIN1 A,B, arrows illustrate elongation of ductal cells with minimal nuclear deformation highlighting precancerous condition. PanIN 2 arrows indicate loss of mucous epithelium, nuclear crowding, and mitotic figures. PanIN3 corresponds to pseudopapillary formation and carcinoma, high nuclear pleomorphism, and intraluminal debris. Figure from (Makohon-Moore, 2016).

Most pancreatic cancers occur sporadically, with several molecular profiling studies illustrating the mechanisms involved in the established PanIN-to-PDAC progression model (Makohon-Moore, 2016). Histological aspects of PanIN transformations and staging are classified into three grades: low grade lesions with minimal architectural dysplasia designated as PanIN-1A (flat) and PanIN-1B (papillary), intermediate grade PanIN 2 with nuclear crowding and moderate atypical cytological appearance, and high grade PanIN 3 with high nuclear pleomorphism and carcinoma formation (Distler, 2014). Genetic mutations correlated to each stage are as follows: low grade PanIN lesions having point mutations in the Kras oncogene and telomere shortening, intermediate grade having inactivating mutations of cyclin-dependent kinase inhibitor 2A (CDKN2A) necessary in controlling cell cycle regulation, and high stage showing mutations in

TP53 and SMAD4 (Guo, 2016). Early detection and treatment of these precursor lesions could probably save patients from advancing to invasive pancreatic cancer (Pittman, 2017). However, extensive evaluation into the molecular signaling of pancreatic cells undergoing cancerous transformation and progression is needed to further elucidate potential gene targets for therapeutic intervention.

Stromal Environment

Despite pancreatic cancer's association with these specific mutations, therapeutic targeting of these mutations have proven to be clinically ineffective. Stromal cells can account for nearly 90% of pancreatic tumor volume and can contribute significantly to tumor progression. Although various signal transduction pathways and genetic mutations have been identified, there remains a need for development of early detection methods, as well as combining chemotherapeutic with immune targeted therapies towards the microenvironment to control disease progression and survival. Stromal cells of note consist of cancer-associated fibroblasts (CAFs), pancreatic stellate cells (PSCs), myeloid derived suppressor cells (MDSCs), as well as large populations of macrophages and neutrophils/polymorphonuclear leukocytes (PMNs) (Nielsen, 2016).

PSCs are essential to extracellular matrix formation and maintenance under normal conditions. The balance of this profibrogenic capability is disrupted when PSCs are activated by cancer cells to become cancer-associated human PSCs (CA-hPSCs) that promote chemoresistance, local tumor progression, and metastasis (Philips, 2012). The cumulative effects of disease onset by compromised cells release increased levels of cytokines, reactive oxygen species (ROS), and growth factors which stimulate quiescent PSCs to increase expression of α-smooth muscle actin (α-SMA) (Koikawa, 2018). The degree of PSC and graded fibrosis activity has been indicated as a stromal activity index, a ratio of α -SMA to the density of collagen deposition which can be visualized via immunohistochemical analysis (Fig. 2). This potential

prognostic tool was evaluated in a study with 233 post-surgical pancreatic cancer patients where high stromal activity index scores were positively correlated with low prognosis (Erkan, 2008). In-vivo xenograft models using nude mice evaluated the ability of CA-hPSCs to protect pancreatic cells in mice which received subcutaneous injections of solely human pancreatic cells or in combination with human PSCs (Mantoni, 2011). Results of this study showed tumor growth was more pronounced in those formed from both human PSCs with pancreatic cells in response to radiation therapy, versus those formed only from pancreatic cells alone (Mantoni, 2011). Collectively, the role of CA-hPSCs in pancreatic cancer chemoresistance and progression is paramount to cancer cell survival. Thus, reducing the activity of CA-hPSCs by better understanding their survival mechanism may reduce the aggressiveness of PDAC.

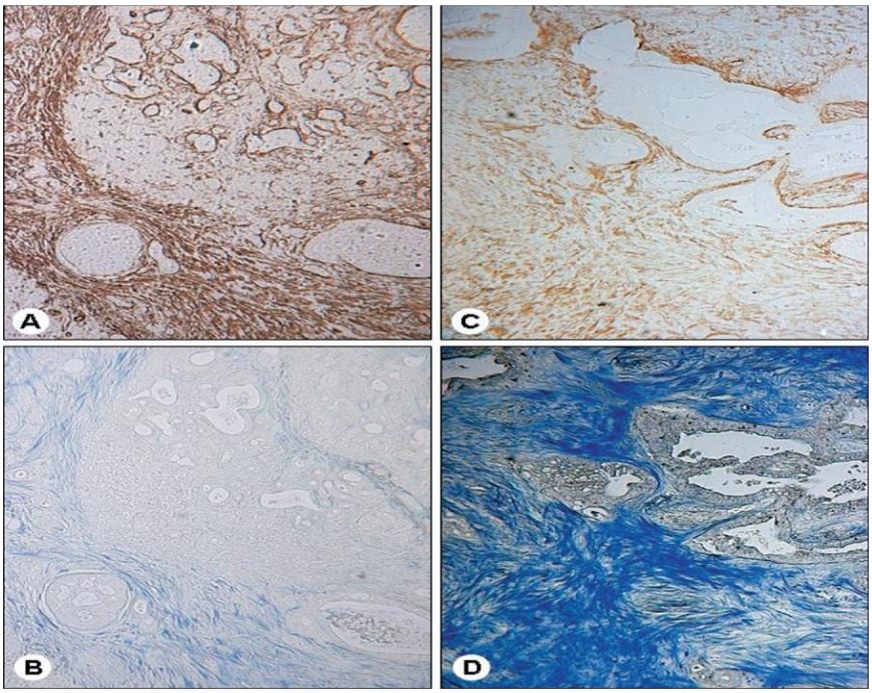

Figure 2| Immunohistochemical analysis comparing collagen deposition versus stellate cell activity around cancer structures. Immunohistochemistry performed using an anti-SMA antibody (brown) to detect activated PSCs and aniline (blue) to stain collagen fibers (B and D). (A and C) Density of activated PSCs increased around cancerous (unstained) structures. (A and B) Areas of activated PSCs colocalized with collagen deposition. (C and D). Image by (Erkan, 2008).

Neutrophil Development

Being the most abundant white blood cells (WBCs) to an immune response, neutrophils account for 50-70% of leukocyte populations. Under normal physiological conditions, neutrophils act as first responders to inflammation and infections that is resolved by macrophages. Granulopoiesis, the process of neutrophil development, occurs predominantly in the bone marrow. During granulopoiesis, long-term hematopoietic stem cells (LT-HSC) differentiate into short-term hematopoietic stem cells (ST-HSC) followed by multipotent progenitor (MPP) cells (Nicolas-Aliva, 2017). Neutrophil differentiation, under the influence of granulocyte-colony stimulating factor (G-CSF), then continues through the subsequent stages: lymphoid-primed multipotent progenitors (LMPPs) GMP, myeloblast, promyelocyte, myelocyte, metamyelocyte, band neutrophil, mature neutrophil, and finally segmented neutrophil as illustrated in (Fig. 3)

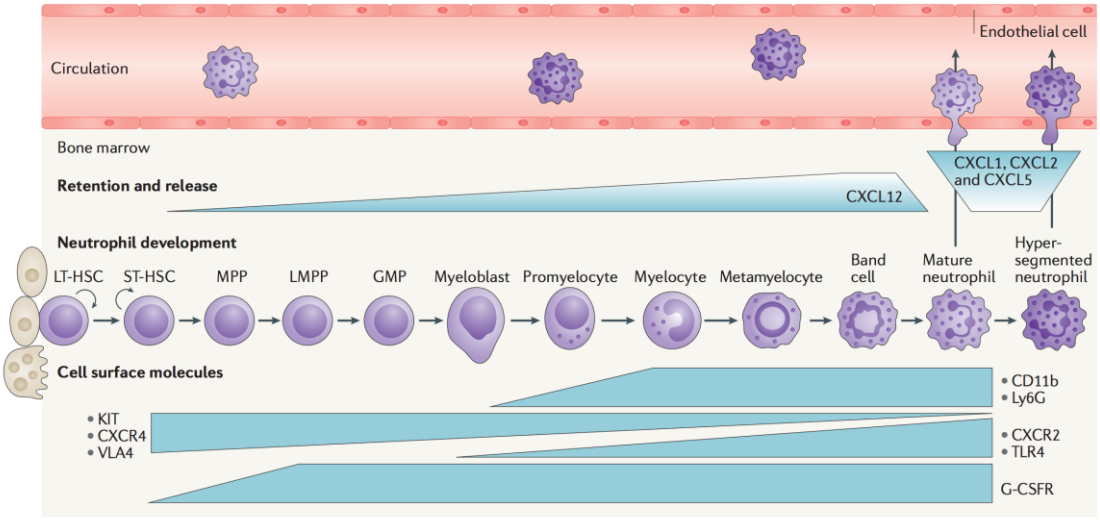

Figure 3 |Hematopoietic development of neutrophils. The development of neutrophils from long term hematopoietic stem cells (LT-HSC) to ST-HSC, MPP, LMPP, GMP, Myeloblast, promyelocyte, myelocyte, metamyelocyte, band cell and mature neutrophils. Cell surface molecule expression levels fluctuate dependent on stage of development. Ligands to CXCR4 retain neutrophils, while, CXCR2 recruit mature neutrophils out into circulation. Image by (Coffelt, 2016).

Neutrophils contain an abundance of antimicrobial compounds stored within granules. Throughout their developmental stages, neutrophil granules begin to appear at distinct stages. Primary (azurophil) appear between the myeloblast to promyelocyte stages, secondary (specific)

granules appear between the myelocyte to metamyelocyte stage, tertiary (gelatinase) granules take on appearance during the band cell to segmented stages (Coffelt , 2016). As neutrophils mature, they down regulate expression of various receptors such as KIT and C-X-C chemokine receptor 4 (CXCR4), while upregulating others such as CD11b, Ly6G in mice, CXCR2 and Toll-like receptor 4 (TLR4) (Coffelt, 2016). Mature neutrophils, primed for mobilization into circulation, express ligands for CXCR 2, which include CXCL2, CXCL5, and CXCL8. Of note, CXCL2, and CXCL5 are known to mobilize mature and hypersegmented neutrophils out of the bone marrow and egress into the bloodstream. Primarily, chemokines regulate the balance between neutrophil retention and release. Bone marrow stromal cells produce CXCL12 that binds CXCR 4, leading to neutrophil retention, while release is controlled mainly by CXCR2 signaling (Nywening, 2017). Circulating mature neutrophils have a short life span of several hours to one day before undergoing apoptosis either at distant tissue sites or after returning to the bone marrow (Borregaard, 2010).

Neutrophil Immune Response In Disease

Neutrophil mechanisms for neutralizing pathogens involve: 1) degranulation of bactericidal enzymes, including myeloperoxidase (MPO), neutrophil elastase (NE), and cathepsin G, 2) release of reactive oxygen species (ROS), also known as oxidative burst, and 3) release of web-like decondensed nuclear DNA called neutrophil extracellular traps (NETs), a process called NETosis (Fig. 4).

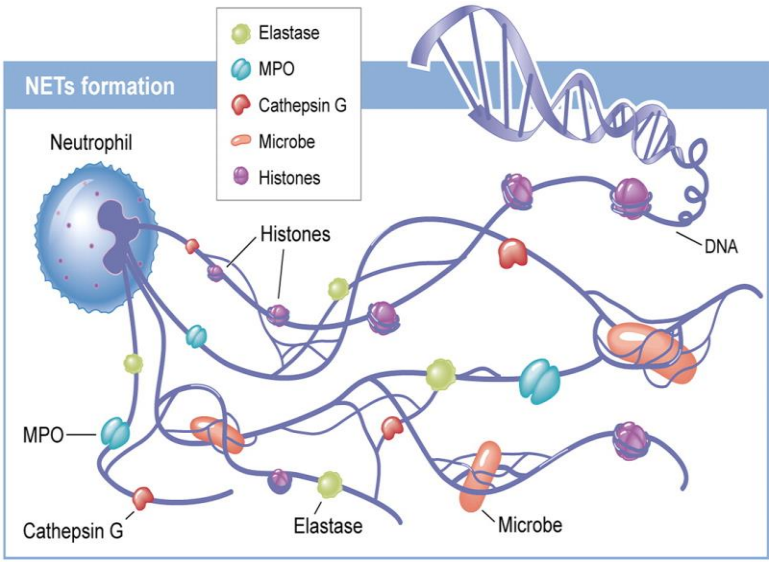

Figure 4|Net Formation. Illustration of active neutrophil undergoing NETosis. Expelled decondensed DNA contains various proteases including neutrophil elastase (NE, myeloperoxidase (MPO), cathepsin G, and histones in response to microbial pathogens. Figure by (Miyata, 2012).

NETs are a classical cytotoxic response characterized by chromatin decondensation (induced by peptidyl arginine deiminase 4 (PAD4) histone citrullination), dissolvement of the nuclear and granule membranes, and mixing of chromatin and granule enzymes that are secreted as a sticky meshwork for trapping and killing bacteria (Merza, 2015). NETosis is stimulated by phorbol-myristeacetate (PMA), lipopolysaccharide (LPS), interferon-gamma(IFN-γ), and microbial pathogens (Almyroudis, 2013). NETs contain an arsenal of granular proteases such as serine-proteinase neutrophil elastase (NE), matrix metalloproteinases MMP-8 and MMP-9, and myeloperoxidase. The NADPH oxidase enzyme in neutrophils is also associated with NET formation. Activation of neutrophils through the recognition of various pathogenic stimuli, activates the NADPH oxidase complex through protein kinase C (PKC)/Raf/MERK/ERK, as well as increases in cytosolic Ca^{2+} levels which act as cofactors for PAD4 (Lewis, 2015) (Fig. 5).

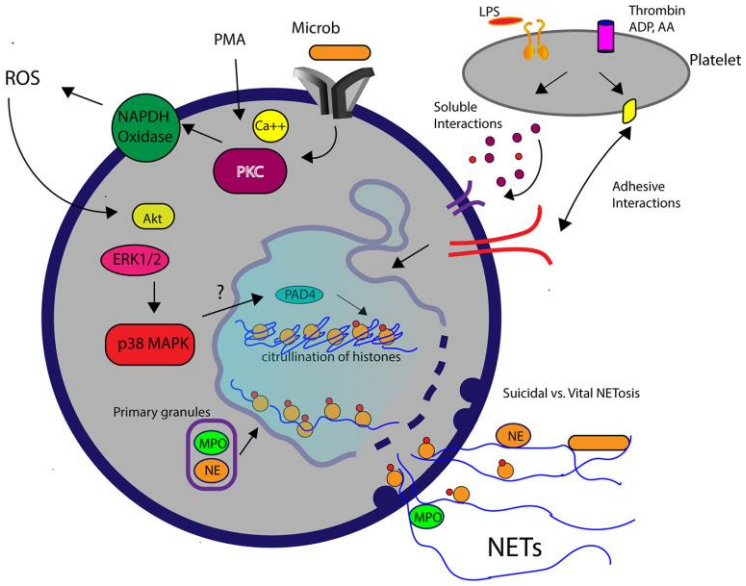

Figure 5| Molecular pathways involved in NETosis. Microbial interaction with pathogen recognition receptors or phorbol-myristeacetate (PMA) induced elevation of intracellular calcium on neutrophils subsequently activates protein kinase C (PKC) and NAPDH oxidase. Reactive oxygen species (ROS) generated by NADPH oxidase leads to downstream signaling mediated by Akt, extracellular signal regulated kinase (ERK1/2) and p38 mitogen-activated protein kinase (MAPK). Chromatin decondensation requires relocation of myeloperoxidase (MPO) and neutrophil elastase (NE) into the nucleus and histone citrullination (citH3), mediated by peptidylarginine deiminase 4 (PAD4). Activated platelets in response to lipopolysaccharide (LPS) or agonists such as thrombin can stimulate neutrophils to produce NETs via soluble or cell-mediated interactions. Image from (Boysen, 2018).

More recently, PADs have been implicated as critical mediators of NETosis and serve as a potential target for NET associated diseases. There are five peptidyl arginine deaminases (PAD) which consist of PADs 1,2,3,4, and 6. PADs 2 and 4 are the only two involved with hematopoietic cell lines, thus play an important role in signaling process of the immune system (Vossenaar, 2003). Although expressed by some cancers, PAD4 is primarily expressed by granulocytes and its activity is calcium dependent (Merza, 2015). Histone citrullination by PAD4 aids in NET formation by promoting decondensation of the chromatin structure and ejection of DNA and is critical to neutrophil response to pathogenic infection (Rohrbach, 2012). This was shown using $PAD4^{-/-}$ mice (Hemmers, 2011) in which $PAD4^{-/-}$ neutrophils were unable to produce NETs due to reduced histone citrullination and, as a result, increased susceptibility to microbial infection (Li, 2010*)*

The generation of NETs can produce varied effects. On the one hand, they may promote pathogen killing. However, the same pathways that control microbial infection can also cause injury through several mechanisms. NET products can damage epithelial and endothelial cells, which can exacerbate inflammation induced organ injury (Saffarzadeh, 2019). This highlights the importance of NETs in autoimmune and autoinflammatory pathologies, such as rheumatoid arthritis, systemic lupus erythematosus (SLE), vasculitis, lung injury, atherosclerosis, and thrombosis (Kruger, 2015). Several strategies have been proposed to interfere with NETs, particularly digestion of NET DNA with DNase1, targeting NET-associated proteins, and PAD inhibitors (Jones,2009). Due to their potential role in human disease, PAD inhibitors are of high interest. For example, the compound Cl-amidine, acts via irreversible inhibition by preferentially inactivating the calcium bound form of the enzyme (Biron, 2017). In a mouse model of SLE, systemic treatment with the PAD4 inhibitor, BB-Clamidine, was shown to protect mice from developing NET-mediated vascular damage, endothelial dysfunction and kidney injury (Knight, 2013). Sepsis models demonstrated that PAD4 deficiency in $PAD4^{-/-}$ mice improved overall survival and showed decreases in organ dysfunction without exacerbating bacteremia (Biron, 2018). Nonetheless, due to the physiological complexities of systemic PAD4 inhibition, developing a suitable targeted therapy for PAD4 remains to be seen.

Tumor Associated Neutrophils

In recent years, neutrophils have received more attention in the context of tumorigenesis driven by inflammation. Within this context is the concept that tumor associated neutrophils (TAN) are believed to have differential activation states which correspond to anti-tumor or pro-tumor effects (Nicolas-Aliva, 2017). This is believed to be a result of overexpression of several cytokines. Of note, TGF-β has been highlighted as having protumor effects via its release and interaction within the microenvironment. Neutrophils acquire phenotypes which are protumor (N2 TAN) induced primarily by the accumulation of TGF-β in the microenvironment, and anti-

tumor (N1 TAN) that are induced by the presence of low TGF-β and high IFN-y (Felix, 2016). N2 TANs promote invasion, growth and metastasis through degradation of the extracellular matrix (ECM), angiogenesis, and immunosuppression, while N1 TANs abrogate tumor progression through tumor cell toxicity and enhancement of the antitumor immune memory response (Piccard, 2012). Concurrently, TGF-β has been shown to impact myeloid cell functions by polarizing macrophages to become protumor (M2) versus antitumor (M1) (Fridlender, 2009). An important distinction to note is that unlike M2 tumor-associated macrophages which characteristically express CD206, there are no clear cell surface markers distinctive to TANs which exhibit cell plasticity and tissue context dependent functions, (Meri, 2018).

In proinflammatory diseases, certain proteases derived from neutrophil granular enzymes such as NE and MMPs, can modify the ECM, a phenotype shown to contribute to cancer progression by degradation of the basement membrane. (Swierczak, 2015). NE is stored in primary azurophilic granules with its antimicrobial action being counterbalanced primarily by α1-antitrypsin and other natural inhibitors. An imbalance between NE and its inhibitors has been implicated in tumor development such as liver, lung cancers, and increased concentrations of NE in cancers has been correlated with poor survival (Sun, 2004). Using a mouse model of lung adenocarcinoma of Kras activation, one study showed that NE expression increased lung tumor growth and decreased overall survival time in Kras/NE positive mice when compared to Kras/NE deficient mice (Houghton, 2010). This same study further indicated that NE has a direct effect on inducing tumor cell proliferation. NE effects on proliferation were dosage dependent in which higher concentrations induced cell death, and moderate concentrations resulted in cell proliferation (Houghton, 2010). Of note here is that NE concentration levels could relate to neutrophil activation states and the need for further study as to how these differential states are influenced by the tumor microenvironment.

MMPs are the primary factors which function to degrade the ECM. Overexpression of MMP-2 and MMP-9 in pancreatic cancer was previously reported**,** and these gelatinases were also investigated as differential markers for chronic pancreatitis (CP) and PDAC (Wang, 2019). For instance, MMP-9 expression by TANs promotes angiogenesis and cleavage and activation of CXCL8 which is expressed by tumor cells (Nicolas-Aliva, 2017). Furthermore, MMP-9 cleaves the substrate endothelin ET-1(AA 1–38) into ET-1(AA 1–32) which activates neutrophils and promotes leukocyte-endothelial cell adhesion and subsequently, neutrophil trafficking into targeted areas of inflammation (Iyer, 2012). Other studies have shown that neutrophil derived MMP-9 is a direct inducer of pancreatic tumor angiogenesis. Together, these observations suggest that PMN derived MMP-9 has a direct proangiogenic effect and is essential for tumor-associated blood vessel formation and tumor growth (Deryugina, 2015).

Neutrophils in Pancreatic Cancer

During infections, chronic inflammation, and malignancies neutrophil are systematically expanded in the bone marrow, released into circulation and recruited to the site of disease or tumor in response to chemotactic factors such as granulocyte-macrophage CSF (GM-CSF), G-CSF, or neutrophil- attracting CXC-chemokines (Gabrilovich, 2012). Once in circulation, cell adhesion molecules located on neutrophils surface (CD11b) as well as adhesion molecules on the surface of blood vessel endothelial cells (selectins, ICAM-1 and PECAM-1) are crucial in the rolling, adhesion, and transmigration of the neutrophils from the bloodstream into the tumor (Cerutti, 2017).

Upon infiltration into the pathogenic site, neutrophils join a diverse desmoplastic cellular stroma of the microenvironment that consists of cells such as macrophages, anti-inflammatory myeloid-derived suppressor cells (MDSCs), as well as stellate cells, fibroblasts, and hematopoietic progenitor cells (Makohon-Moore, 2016). In an orchestrated fashion, these mediators create an environment conducive for tumor growth, proliferation, malignant

transformation, and progression (Kruger, 2015). In addition, granulocytic MDSCs interfere with T-cell proliferation (Fig. 6).

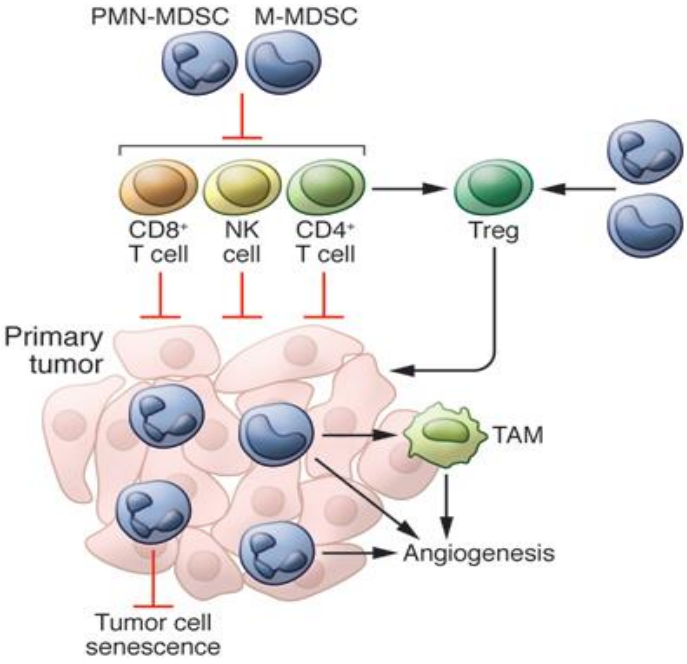

Figure 6| Potential role of monocyte and neutrophil associated myeloid suppressor cells (MDSCs) in the regulation of tumor development and progression. Tumor development is associated with the expansion of cells with acquired immunosuppressive activity (MDSCs). These cells also promote tumor cell invasion and angiogenesis and neutralize tumor cell senescence. Image by (Marvel, 2015).

A mechanism of MDSC immune suppression includes release of reactive oxygen species (ROS), arginase-1 (arg-1), and nitric oxide (NO) (Porembka, 2012). More recently, it has been shown that peroxynitrite (PNT), created as a byproduct of NO and superoxide interactions, could cause nitration of T cell receptor-CD8 complex which reduced its binding to the peptide MHC class I (pMHC) complex, and rendered T cells unresponsive to antigen-specific stimulation (Marvel, 2015). These effects illustrate the promoting effects stromal cells have on tumor progression. In line with this, neutrophil recruitment and infiltration into cancer exacerbate disease progression.

As discussed previously, TANs play an important role in cancer development, progression, and resistance to therapy. In relation to PDAC, large numbers of TANs have been

strongly correlated with poorer prognosis (Reid, 2011). High intratumoral CXCL5, a chemokine for neutrophils, have also been associated with poorer overall survival (Hu, 2018)). In a KPC mouse model, GR1+ myeloid cells, which includes neutrophils, were depleted using mAbs and showed increased infiltration of effector T cells and inhibited tumor growth (Stromnes, 2014). Therefore, targeting neutrophils may be therapeutic in PDAC. CXCR2 ligands are essential for neutrophil egression from the bone marrow and trafficking toward sites of inflammation and for the recruitment of TANs in various cancers (Fu, 2018). The importance of high infiltration of TAN has been used to assess patient prognosis in relation to neutrophil/lymphocyte ratios.

As discussed previously, TGF-β is known to drive neutrophils toward a protumor (N2) phenotype. Notably, platelets are an abundant source of TGF-β, and platelets activated by tumor cells contribute further to microenvironment concentration of TGF-β (Olson, 2018). Recent studies have explored the contribution of tumor-induced platelet activation and coagulation in pancreatic cancer progression (Maugeri, 2014). Platelets in contact with tumor cells induced metastasis by activating platelets to secrete CXCL5 and CXCL7 which are known neutrophil chemoattractants. Activated platelets induce NET formation by stimulating neutrophils via cell mediated binding of von willebrand factor (vWF) to CD18 on neutrophils as well as soluble factors high mobility group box 1 (HMGB1) and platelet factors 4 (PF4) (Fig. 7) (Cartesia, 2016). NET histones elicit procoagulant activity providing a scaffold for thrombus formation and growth (Jurasz,2004). Providing answers to these cell interactions will require an improved understanding of the dynamic interaction between cancer cells and their stroma in designing new, effective therapeutic strategies for pancreatic cancer.

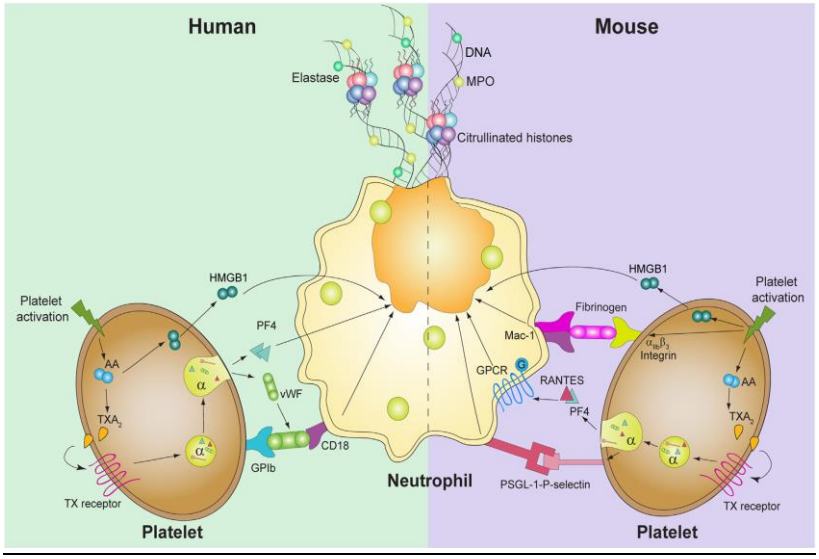

Figure 7| Activated Platelet Neutrophil NETosis interaction. In humans (left), platelet activation induces thromboxane A2 (TXA2) formation. This activates release of high mobility group box 1 (HMGB1), platelet factor 4 (PF4), and von Willebrand factor (vWF). CD18 on neutrophils is bound to both vWF, bound to its platelet receptor, and glycoprotein (GP)lb. In mice (right), platelet induced NET formation is carried out through G-protein coupled receptors (GPCR) via HMGB1, PF4, as well as thromboxane 2 (TXA2) PF4 and RANTES. Additionally, binding between P-selectin expressed on platelets and PSGL-1 receptors on neutrophils, is also required for the release of NETs. Figure reproduced from (Carestia 2016)

Potential Therapeutic Targets in Pancreatic Cancer

In PDAC, clinical efforts to utilize immune therapy have been shown to be largely ineffective (Feng, 2017). While patients with other cancers benefit from increased survival rates with immunological check-point inhibitors enhancing anti-tumoral immune cell activity, only small subsets of PDAC patients respond to these treatments (Le, 2017). Thus, a major constraint is placed on immunotherapeutic strategies aimed to address PDAC. In comparison, infiltration of CD8+ tumor infiltrating leukocytes (TILs) into the tumor stroma has been identified as an important element in determining long-term survival in PDAC patients. Miksch et al., studied the importance of peritumoral tumor infiltrating leukocytes (CD3+, CD8+, CD20+ TILs, and CD66b+ tumor infiltrating neutrophils (TINs), to better understand these cell populations in relation to patient prognosis (Miksch, 2019). This group found that high infiltration of CD3+, CD8+, and CD20+ TILs was associated with improved overall and progression-free survival (Miksch, 2019). These results show promise, but a combination of approaches will be necessary

in order to combat the dense fibrotic PDAC tumor stroma and the immunosuppressive microenvironment which act to impede antitumoral immune response (Puleo, 2018).

Multiple clinical trials have failed to demonstrate efficacy simply due to the aggressive nature of PDAC, with further impediments posed by the immunosuppressive tumor microenvironment (Manji, 2017). Furthermore, the dense stroma and rigid ECM architecture restricts effector immune cells from reaching their tumor sites in a phenomenon known as excluded infiltrate tumor microenvironment (Watt, 2013). Understanding the interconnected pathways and interactions between cells both systemically and within the stromal site will be crucial in designing clinical trials with improved clinical outcomes. Cancer cell interactions with the immune system is comprised of the following three phases: elimination, equilibrium, and escape phases (Mitall, 2014). First, the immune system recognizes and eliminates transformed cells. Transformed cells that escape the elimination phase then enter the equilibrium phase, in which the cancer cells undergo genomic editing and establish the tumor microenvironment that supports the growth of early neoplastic cells (Mitall, 2014). Finally, in the escape phase, cancer cells recruit immunosuppressive cells like MDSCs, tumor associated macrophages (TAMs) and regulatory T-cells, (Treg cells) (Wargo, 2016). In spite of such obstacles, studies have supported the viability of immunotherapeutic approaches to render cancer cells vulnerable by restoring the immune systems anti-tumor capability and response.

Antibody-mediated immunotherapy involves targeting tumors to inhibit oncogenic signaling, immune suppression by using monoclonal antibodies (mAbs), antibody-drug conjugates, or radioimmunotherapy conjugates (Vonderheide, 2013). CD40 is a member of the tumor necrosis factor (TNF) receptor superfamily and is expressed primarily on antigen presenting cells (APCs) such as dendritic cells (DCs), macrophages, monocytes, B-cells and some non-immune cells like cancer cells (Amarsaikhan, 2017). The mechanism of anti-CD40 mAb is to activate host APCs and induce antitumor T-cell responses, reverse tumor induced immune

suppression and induce T-cell independent but macrophage dependent tumor regression in pancreatic cancer patients (Torphy, 2018). One clinical trial with 22 patients who had advanced staged pancreatic cancer, showed increased B-cell surface expression of costimulatory molecules CD86, human leukocyte antigen complex (HLA-DR), and CD54 at 24-48 hours post-treatment when given weekly doses of gemcitabine in combination with anti-CD40 mAb, (Vonderheide, 2013). In a clinical trial with 21 surgically incurable pancreatic cancer patients, three-week cycles of treatment with gemcitabine and a human agonist anti-CD40 mAb showed increased overall survival of 7.4 months compared to those who received gemcitabine alone with average overall survival of 5.7 months (Bekaii-Saab, 2017).

Combination therapies have gained traction by having shown some success in two or three drug combinations. The international phase III clinical trial (NAPOLI-1) study compared combination nanoliposomal irinotecan, leucovorin, and infusional 5-fluorouracil (5-FU) (5-FU/nal-I) with leucovorin and infusional 5-FU alone and with nal-I alone after failure of gemcitabine-based therapy. The combination regimen was significantly better than 5-FU, prolonging mean overall survival from 4.2 to 6.1 months (Wang-Gillam, 2016). Consequently, the extent of trials employed to combat cancers illustrates the robust measures that tumors must escape in immune surveillance and progression. This would suggest that development of strategies to counteract and improve efficacy will require a combination of conventional treatment options, while reevaluating other potential therapeutic targets to improve patient survival. One such avenue involves studying the effect of neutrophil NETs on pancreatic cancer progression.

Pancreatic cancer is an aggressive disease with a high mortality rate. The stromal microenvironment in this disease is composed of various cells that can promote tumor proliferation, progression, and metastasis. Concurrently, recruitment of immune suppressive cells

allows the cancer to evade immune detection and continue to grow. Highly influential in tumor progression and survival are neutrophils and their antimicrobial components that are comprised in NETs to normally fight disease, but when become tumor associated, can provide a survival advantage for cancer. Dysregulation of NET formation and the mechanisms behind its induction as well as neutrophil communication with other cancer associated cells within the microenvironment, provide avenues for novel strategies that combat disease. These include improving early detection strategies, bolstering antitumor immune responses, and development of combination therapies to target multiple components of disease initiators, while maintaining healthy immune function and patient tolerability to treatment in order to improve overall survival.

Hypothesis

Neutrophils impact pancreatic cancer proliferation and metastatic capability through NET mediated mechanisms.

Chapter 2: Materials and Methods

Cell Culture

MiaPaca-2 (primary tumor) and Capan-1(liver metastasis) cells, obtained from Dr.Rakesh Singh's lab group at the University of Nebraska Medical Center (UNMC). S2007 (lung metastasis) and S2013 (liver) were sublines cloned invitro from a human pancreatic cancer cell line (SUIT-2), along with AsPC1 (ascites fluid) were provided by the Hollingsworth group at UNMC. All cells were cultured as monolayers in T75 flasks. MiaPaca-2, AsPC1, and S2013 cell lines were grown in RPMI 1640 (Hyclone) medium supplemented with 10% fetal bovine serum (FBS), penicillin (100 ug/ml) and streptomycin (100 ug/ml). Capan-1 cells were cultured in RPMI, 15% FBS, penicillin (100 ug/ml) and streptomycin (100 ug/ml) at 37^{o}C in a humidified incubator with an atmosphere of 5% CO_2.

Preparation of Serum-Free Conditioned Medium

Cells were cultured in T-75 flasks and grown to 75% confluence with 10ml of appropriate cell culture medium prior to application of serum-free RPMI medium. After 24 hours, serum free conditioned medium was collected in a 15ml conical tube and spun down at 2000 rpm for 5 minutes to separate any cells contained within the medium. Following centrifugation, supernatant was collected and conditioned medium (CM) stored in 15ml conical tubes at 4^{o}C. Next, 20ul aliquots of conditioned medias were taken for colorimetric detection and quantitation of total protein using Pierce BCA Protein Assay Kit (Thermo Fischer Scientific). Accordingly, protein concentrations were determined and reported with reference to standards of a bovine serum albumin (BSA) for use in subsequent neutrophil NET Sytox Green experiments.

Isolation and Purification of Mouse Bone Marrow Neutrophils

Mice were euthanized in the University of Nebraska Medical Centers animal facility with 70% ethanol used to sterilize surfaces. An incision was mid within the mid-abdomen and skin

removed from the distal part of the mice, including the skin covering the lower extremities. Muscles were detached from lower extremities using scissors and the acetabulum of the hip join was carefully dislocated to prevent breaking of the femur head. Remaining muscles were removed from the 2 femurs and 2 tibias with scissors and the femurs and tibias were separated at the knee joint to prevent breaking of the bone ends. Bones were placed in 15ml conical tubes containing ice cold 10%PBS. The tube was transferred to a tissue culture hood for sterile technique to avoid neutrophil activation. A 1ml syringe was used to poke a hole at the bottom of four 0.5ml microcentrifuge tubes (Eppendorf) The bones were cut at the epiphyses and each placed inside of 0.5ml microcentrifuge tube to be transferred to 1.5ml microcentrifuge tubes (Eppendorf). The 0.5ml tubes were capped and both tubes transferred to be spun down in a microcentrifuge for 2-3 seconds allowing the bone marrow to flush out into the 1.5ml microcentrifuge tube. The 0.5ml tube containing bones was discarded and four 1.5 ml Eppendorf tubes were transferred back into the hood and bone marrow was gently resuspended with 1ml of Easy Sep buffer. Resuspended bone marrow was pipetted to a 50ml conical tube (Falcon) with a 100um filter and a 10ul aliquot taken for initial cell counting using trypan blue exclusion. The 50ml conical tube was centrifuged at 1,400 rpm for 10 min at 4 degrees Celsius. The supernatant was discarded and resuspended with 1ml cold PBS. In a 15ml conical tube, 3ml of prepared Histopaque 1119 was added and subsequently overlaid with 3ml of Histopaque 1077 on top. 1ml PBS bone marrow cell suspension was slowly overlaid on top of Histopaque 1077 and the tube centrifuged for 30 min at 2,000rpm at 25 degrees Celsius with the brake disengaged. Neutrophils were collected at the interface of Histopaque 119 and Histopaque 1077 layers and transferred to 15 ml round bottom polystyrene centrifuge tubes (Thermo Fisher Scientific). Collected neutrophils were washed 2x in 4ml Easy Sep buffer and centrifuged at 1,400 rpm for 7min at 4 degrees Celsius. Neutrophils were then counted to determine viability. Typical yields of neutrophils from bone marrow (i.e. 2 femur and 2 tibia bones) of an uninfected 8-12 wk-old

C57BL/6 mouse is approximately 6-12 million cells. For experiments utilizing human derived blood neutrophils, isolations were performed by Yangsheng Yu in Su lab group.

Sytox NETosis Assay

For experimentation, 1ml aliquots of $1x10^6$ neutrophils in RPMI were prepared for the following conditions: complete RPMI, complete RPMI + Phorbol 12-myristate 13-acetate (PMA), MiaPaca-2 CM, Capan-1 CM, AsPC1 CM, S2013 CM. 200uL aliquots of 1ml $1x10^6$ were transferred to one well of a 96 well dark plate (triplicates) and incubated for 2-3 hours at 37^{o}C at 5% CO_2. Following incubation, Sytox green (5uM) was added to neutrophil aliquots and allowed to incubate for 15 min in incubator. Fluorescence analysis was performed with plate reader at 488nm wavelength taken on EVOS FL Auto microscope. NET: Cell quantification was performed using Image J software.

Cell Viability Assay

Pure neutrophils were diluted in RPMI medium to the density of 1×10^6cells/mL/tube and spun down for 5 minutes at 1,400rpm in 3ml round bottom polystyrene tubes with 500ul (performed in duplicates). Neutrophils were then resuspended in RPMI medium, MiaPaca-2, Capan-1, AsPC1, and S2013 conditioned medias. Cell counts were taken using trypan blue exclusion assay at 0hrs, 18hrs, 24hrs, 36hrs.

Coculture with Pancreas Cancer Cells

For coculture experiments, pancreatic cancer cells were each plated onto 24 well plates at concentrations of $4x10^4$ for conditions of cancer cell, cancer cell+neutrophil, cancer cell+neutrophil+NET inhibitor (GSK 484, 10uM); each condition was done in triplicate. 24 hours following initial cancer cell plating, mouse bone marrow derived neutrophils were isolated and resuspended to concentrations of $8x10^5$ /ml in requisite cancer medias per condition. $4x10^5$/ 500ul

aliquots of neutrophils were pipetted onto neutrophil condition wells. 24 hours later all cancer cells were counted using trypan blue exclusion assay.

Immunofluorescence of Rapid Autopsy Samples (RAP)

For immunofluorescent labelling of myeloperoxidase (MPO) and citrullinated H3 (CitH3) by antibodies, RAP sectioned slides were first dewaxed and dehydrated by the following washing steps: xylene (10min, 2x), 100%EtOH (2min, 2x), 90%EtOH (2min), 80% EtOH (2min), 70%EtOH (2min), 50% EtOH (2min), 1xTBST (15min), 1x TBS (5min). Following the dehydration steps, heat induced antigen retrieval was performed using a pressure cooker. Antigen retrieval with Tris-EDTA buffer (10mM Tris Base, 1mM EDTA solution, 0.05% Tween 20, pH 9.0) was chosen for experiments. Prior to using the pressure cooker, 1L of Tris-EDTA buffer was microwaved to reduce the amount of time needed for samples to be in buffer prior to full pressure being reached. Slides were placed in white histology slide holders and filled with hot buffer to fully submerge sample sections. Remainder of buffer was poured in the pressure cooker surrounding the slide holders. Pressure cooker lid was secured and set cooker to “pressure” and selected “high” on settings for a total of 6 mutes. Once pressure was reached, slide holders were removed and allowed to cool on benchtop for 20 minutes. Once cooled, slide sections were circled with PAP pen and immersed in 1x TBS until ready for blocking solution. Sections were covered with blocking solution (10%serum in 1xTBS) and incubated for 1 hour. Following blocking, diluted primary antibodies (1%BSA in TBS) at concentrations of 1:50 (CitH3) and 3.75ul in 500ul (MPO), were pipetted onto sections and allowed to incubate overnight in humidified chamber. The following day unbound primary antibodies were washed 3x in 1xTBST, 10 mins each, with a final 10 min in 1xTBS. Secondary antibodies Alexaflour 488 donkey anti-rabbit (CitH3) and 568 donkey anti-goat (MPO) (Abcam) were diluted 1:1000 in blocking solution and incubated in humidified chamber for 1hr. Following incubation, unbound secondary

antibodies were washed 3x in 1x TBS 10 minutes each. Slides were transferred to 70% EtOH (2min), and then distilled water until ready to mount with Prolong Gold and stored in dark at 4ºC.

MiaPaca In Vivo Experiment

MiaPaca-luc cells were grown to confluency in complete RPMI media. Cells were trypsinized and washed three times with 1X PBS, and filtered using a 70uM filter. Cells were counted and reconstituted to give 300,000 cells per mouse for injection. Athymic Nude mice (NU/J) (Jackson Labs) were anesthetized with isoflurane, and pancreas was injected with 300,000 cells. Mice were allowed to recover, and subsequent treatments began day 3 after injection. Mice were split into 2 groups of 5, and given isotype control antibody or 1A8 (Biolegend). Mice received a dose of 400ug on day 3 given intra-peritoneally, and subsequent doses remained at 200 ug throughout the rest of the experiment. Mice were given D-luciferein ip twice a week and anesthetized and imaged using the IVIS Spectrum imager (Perkin-Elmer). Luciferase signal was quantified using the Living Image Software. Two days prior to termination of the experiment, mice were anesthetized, and ultrasound performed using the Vivo Imaging Sytem 3100. Analysis of data was performed using the Vevo Lab 3.1.1 software for quantification of 3D tumor volume, according to manufactures instructions.

Microscopy

Cancer cells were observed through the EVOS FL Auto Microscope. Immunofluorescent images were captured with Apotome 2 camera via Zen Pro imaging software on Zeiss Axio Imager Z2 microscope. After images were captured, Adobe Photoshop was used for post image processing to adjust contrast and brightness of the images to highlight neutrophil (MPO) and NET (CitH3) localization.

Statistical Analysis

Statistical analysis was completed using Graphpad Prism 8 software. Data was analysed using a one-way ANOVA test to compare significant differences among each of the experimental conditions. T-tests were also used to compare conditions to the control. The data was considered significant if p-values were less than 0.05.

Chapter 3: Results

Effect of primary vs metastatic PDAC on neutrophil survival

To better understand the impact of MiaPaca-2 (primary pancreatic line) with Capan-1 (liver metastasis line) on neutrophil function, first a viability assay was performed in order to test if conditioned medias obtained from each cell line would impact neutrophil survival. Experimental conditions used were RPMI (control), in comparison with MiaPaca-2 and Capan-1 conditioned medias. Neutrophil counts were obtained using trypan blue exclusion assay at time points of 0hr, 18 hr, 24 hr and 36 hrs. Percent fold changes in both Miapaca-2 and Capan-1 showed a decrease in neutrophil cell number within the first 18 hours. Interestingly, at the 24 time point marked increases in both MiaPaca-2 and Capan-1 were seen to have neutrophils doubled. However, these changes were not statistically significant when compared to RPMI control. At the 36 hr time point, >70% of neutrophils were not viable across all three conditions as illustrated in (Fig.8A). These initial results showing that conditioned medias from nonmetastatic cell lines did not show changes in neutrophil survival. Additional metastatic cell sublines S2013 (liver metastatic line) and S2007 (lung metastasis) derived from SUIT-2(liver metastasis), were used in subsequent experiments. These results illustrated in (Fig8.B). These findings show that pancreatic cancer media stimulates neutrophil proliferation although there were no significant differences between metastatic versus non-metastatic cell line conditioned medias.

.

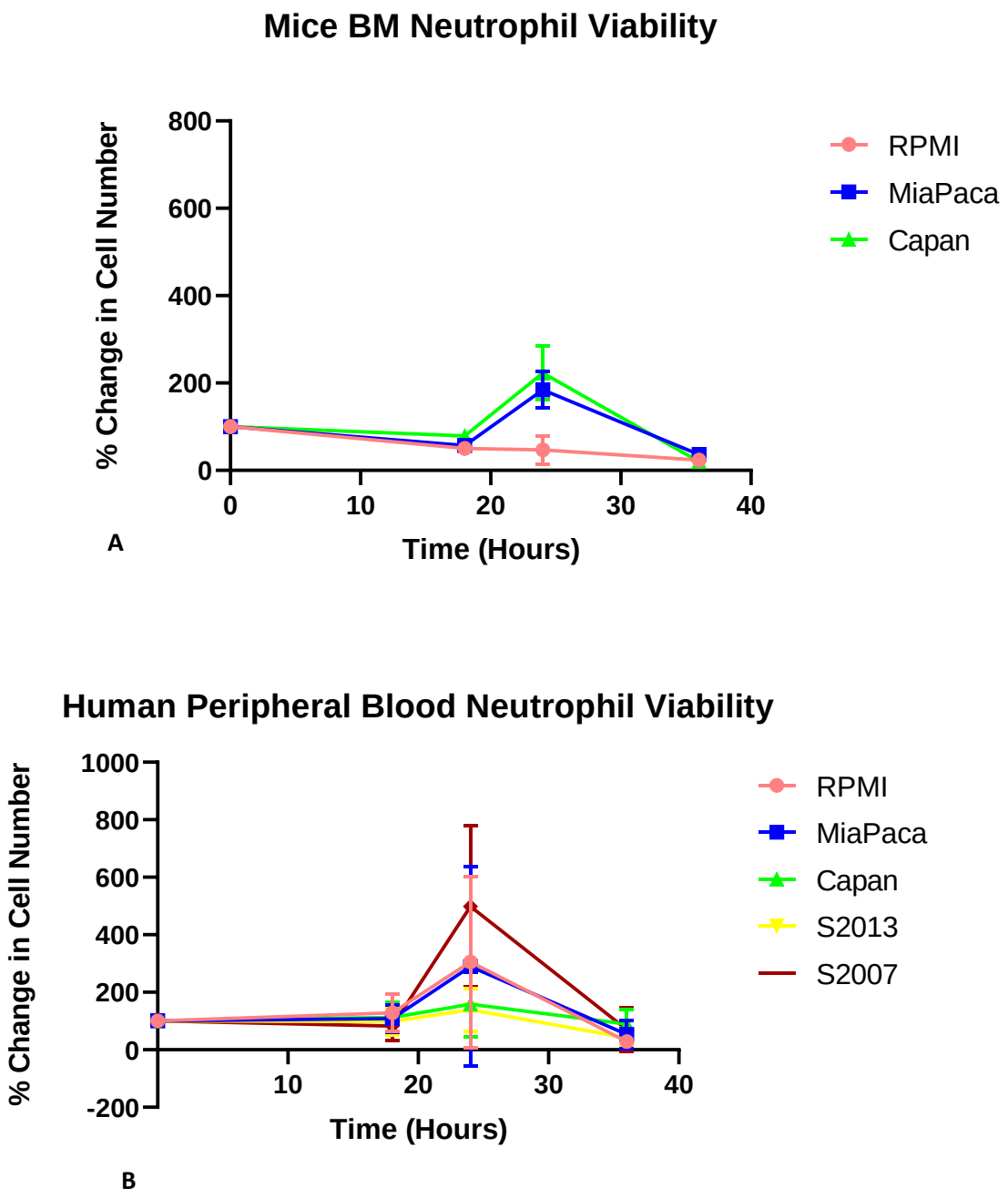

Figure 8| Mouse bone marrow and human peripheral blood derived neutrophil survival assay. (A) Serum free RPMI (control) was compared to MiaPaca-2 (primary tumor cell line) and Capan-1 (liver metastatic cell line) conditioned medias. (B) Serum free RPMI (control) was compared to Miapaca, Capan, S2013 (liver metastasis), and S2007 (lymph node) conditioned medias on neutrophil survival. Time points of 0, 18, 24, 36 hours were used for both experiments.

Primary vs Metastatic PDAC on neutrophil NET formation

To evaluate the impact of primary versus metastatic PDAC on neutrophil NET formation, isolated mouse neutrophils were purified using density centrifugation and cultured in conditioned media from MiaPaca 2 (primary pancreatic line), Capan 1 (liver metastatic line), AsPC1 (nonmetastatic ascites fluid) and S2013 (liver metastatic) cell line conditioned medias. To test the effect of nonmetastatic and metastatic cancer cells on neutrophil NET formation, neutrophils were incubated for 2-3 hours in pancreatic cancer cell conditioned medias. Serum free RPMI media with 2%BSA served as a negative control, while PMA served as a positive control. Extruded NETs were measured using a membrane impermeable dye (Sytox green) that is used to quantify extracellular DNA. Quantification via Styox green indicated varied results between triplicates of experiments. As seen in (Fig. 9A), there was no significance difference seen in between experimental conditions compared to RMPI control. Additional experiments utilizing human neutrophils were done to compare for potential differences in NET formation between mouse and human derived neutrophils in cancer conditioned media. These results illustrate that there were significant increases in NET induction by nonmetastatic vs metastatic conditioned medias (Fig. 9C,D). Particularly, Miapaca-2 conditioned media induced greater NETosis when compared to Capan-1. Concurrently, AsPC1 conditioned media induced greater NET formation than S2013. Based on these results, it was postulated that significant differences in NETosis between metastatic and nonmetastatic conditioned medias may have been resultant of an anti-tumor response. Given this information, further experiments were conducted to investigate the neutrophil impact on pancreatic cancer growth via coculture of neutrophils with nonmetastatic and metastatic cells.

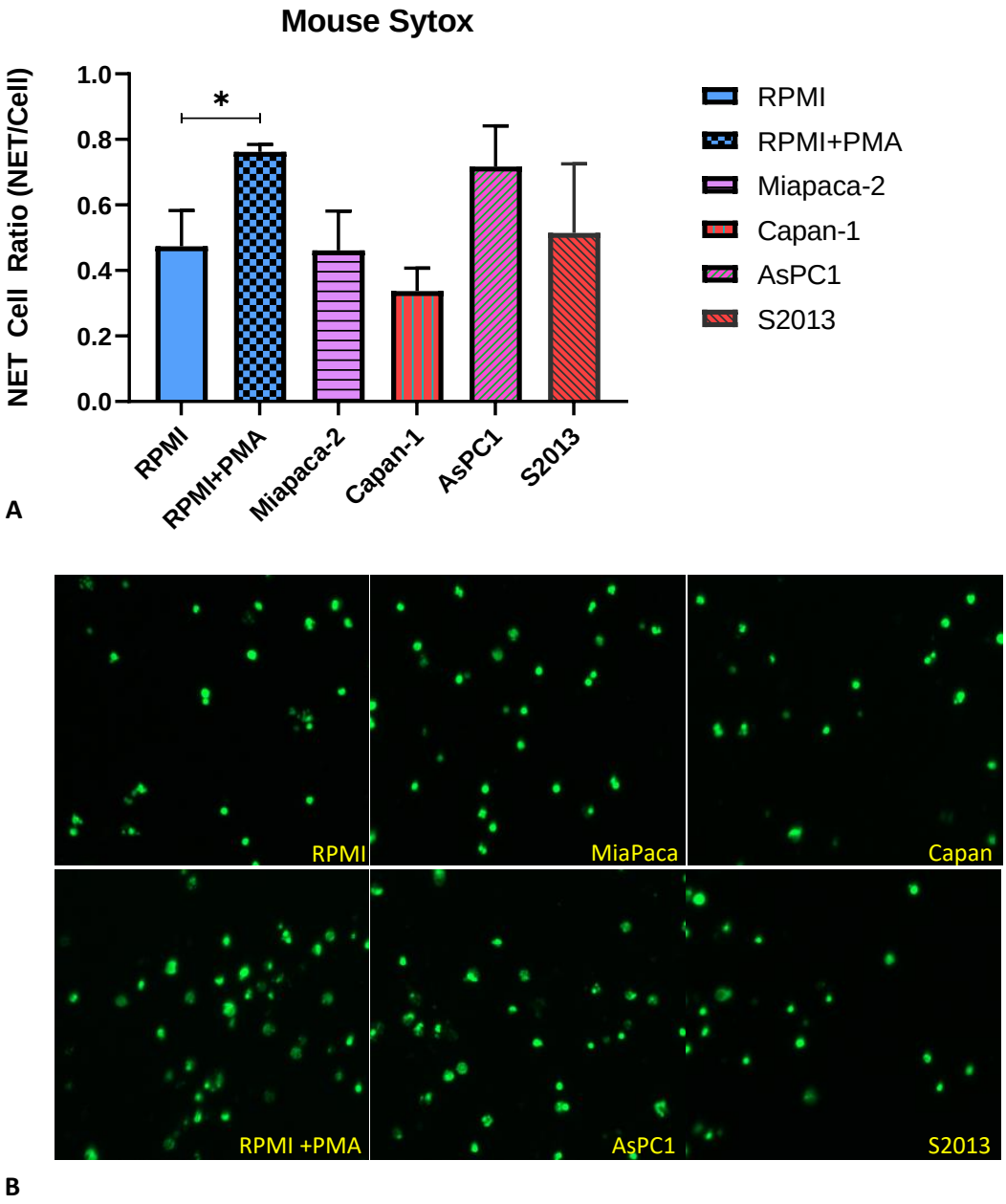

Figure 9 A,B| Induction of NET formation by cancer cell conditioned medias. Neutrophils were isolated and cultured for 4 hours in RMPI+2%BSA, RPMI+2%BSA+PMA, Miapaca, Capan, AsPC1, and S2013 conditioned media all with 2% BSA. (A,B) Mouse neutrophil incubated in pancan conditioned medias.

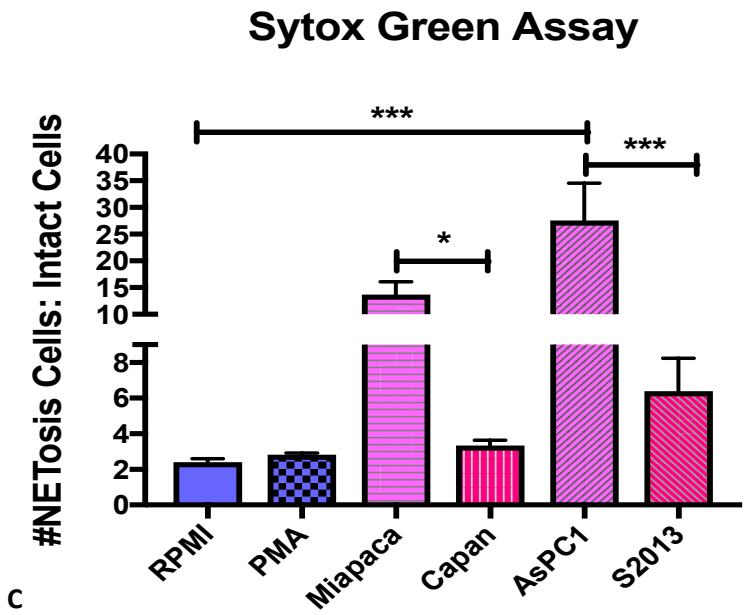

C

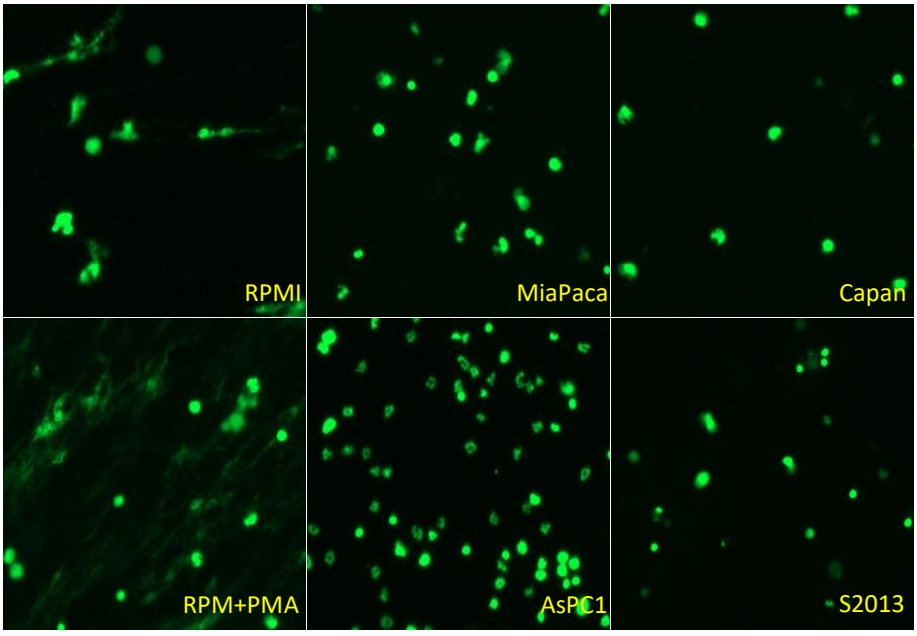

D

Figure 9 D,C| Induction of NET formation by cancer cell conditioned medias. Neutrophils were isolated and cultured for 4 hours in RMPI+2%BSA, RPMI+2%BSA+PMA, Miapaca, Capan, AsPC1, and S2013 conditioned media all with 2% BSA. (C,D) Human neutrophils incubated in pancan conditioned medias.

NET Identification in Patient Rapid Autopsy Samples (RAP)

To evaluate neutrophil infiltration and NET formation in clinical samples, primary and metastatic tumor samples were obtained from post-mortem pancreatic cancer patients who received a combination of chemotherapies, with one group being untreated. Samples were sectioned and stained with myeloperoxidase (MPO) as a measure of neutrophil infiltration and citrullinated H3 (CitH3) to quantify neutrophil NETs. In a sample group of six patients, three sites (pancreas, liver, lung) per patient were tested using immunofluorescence staining. Figure 10A illustrates quantification of neutrophil infiltration (MPO), NET formation (CitH3), and colocalization of neutrophils undergoing NETosis (MPO+CitH3) for each pancreatic and metastatic site. Across all three patients, colocalization counts were comparable in pancreas tumor and lung metastasis, and lowest in liver metastasis. Notably, no statistical significance was seen between the pancreas, liver, or lung groups.

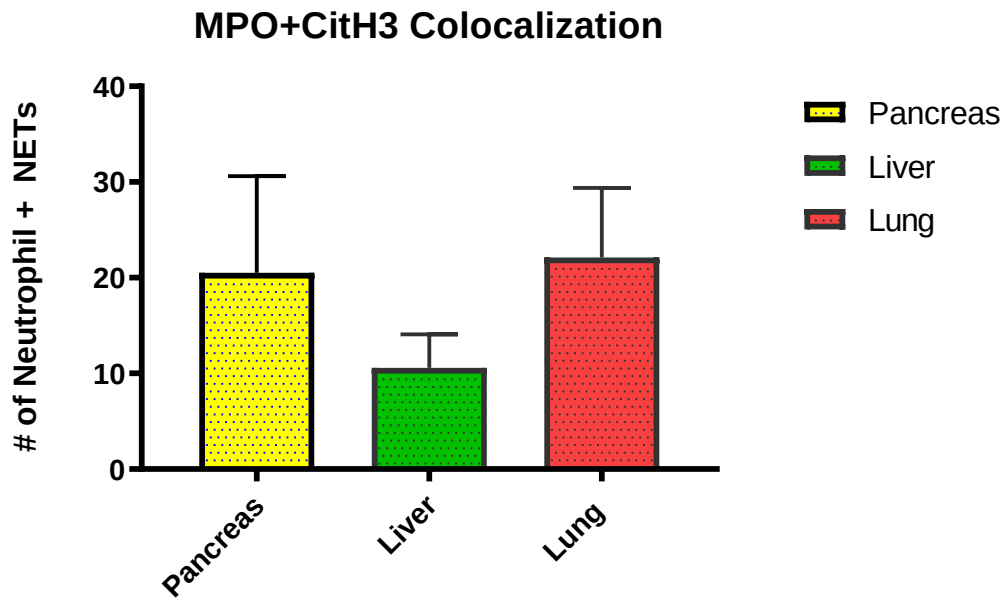

Figure 10A| Representative data illustrating neutrophil infiltration and NETosis colocalization between 6 patients matched samples of pancreas, liver, lungs. Sites of primary tumor and metastasis were patient matched and neutrophils and NETs were quantified via hand counting on Image J software.

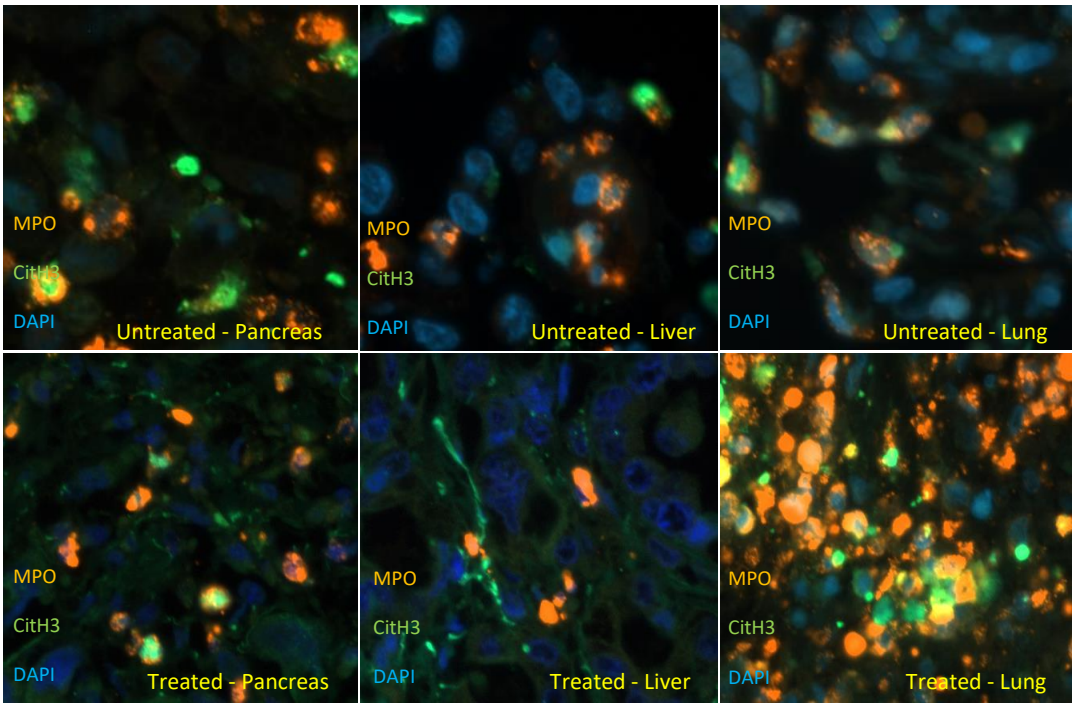

Fig 10B| Representative immunofluorescence images of samples from untreated and chemotherapy treated pancreatic cancer patients with primary tumor, liver and lung metastasis. Cells were fixed, permeabilized and stained for myeloperoxidase (MPO, orange) citrullinated histone H3 (green), and DAPI (blue). NETs were identified by co-localization of (MPO+CitH3).

Impact of Neutrophil NETs on PanCan growth in presence or absence of NET inhibitors

Several recent studies have suggested neutrophil NETs can promote cancer cell proliferation. To understand how neutrophil NETs impact growth of metastatic vs nonmetastatic pancreatic cancer cells, mouse bone marrow neutrophils were isolated by density centrifugation and cultured in-vitro at a concentration of 10:1 (neutrophil: cancer) cell ratio. Other concentrations such as 5:1 and 1:10 were also tested but did not show significant differences in cancer cell killing. Following 24 hours of incubation, trypan blue exclusion assay was used to quantity change in cell growth. Nonmetastatic cell number was decreased by >40% when compared to metastatic cells (Capan-1, S2013), Decreases in cancer cell number were visualized prior to cell counting for gross comparison between conditions (Fig 11). The impact of cancer cell growth was abrogated by addition of GSK484, a PAD4 enzyme inhibitor necessary in NET formation.

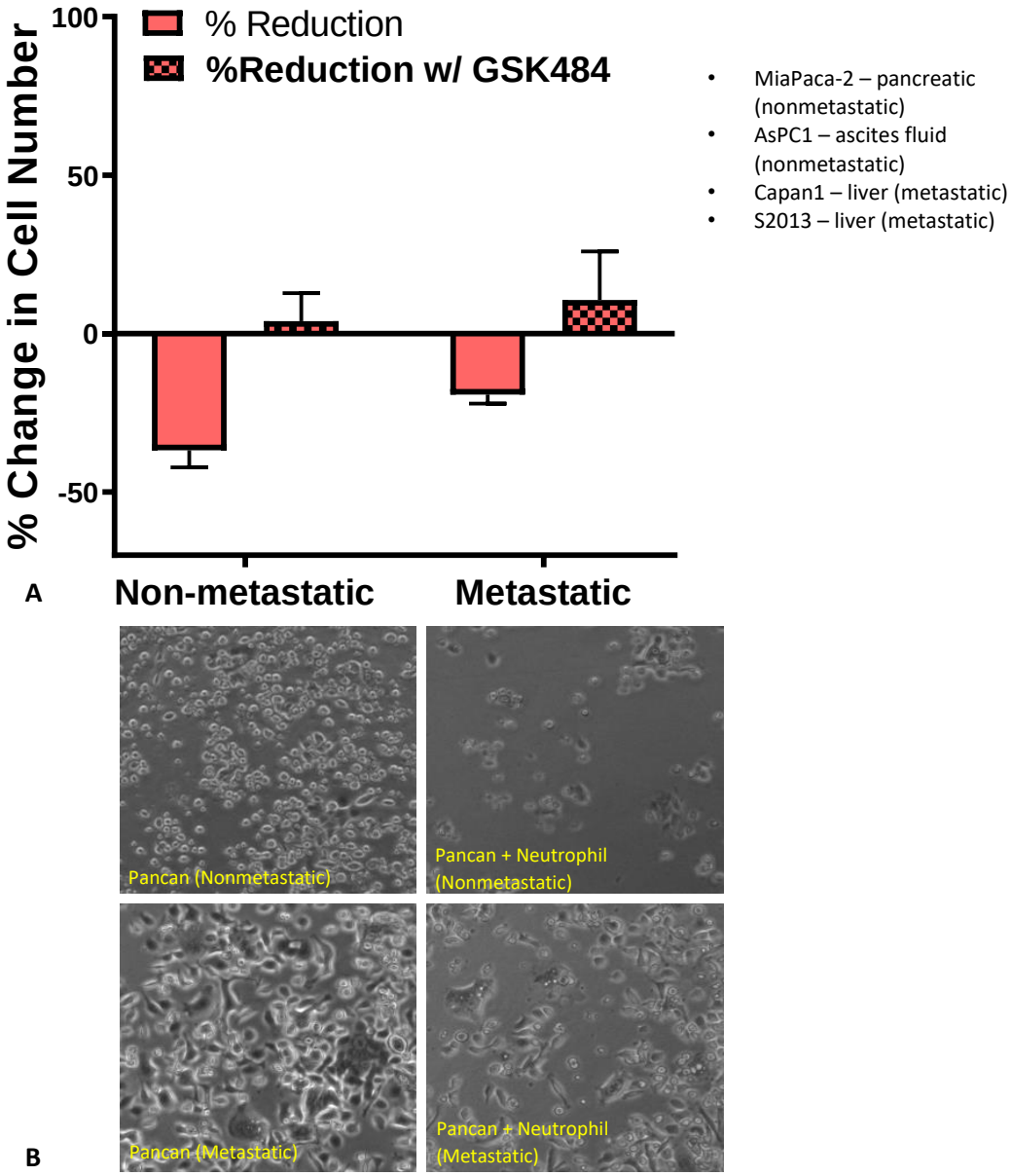

Figure 11| Coculture of Mouse Neutrophils with Pancreatic Cell Lines. Comparison between primary pancreatic lines (MiaPaca, and AsPC1) and metastatic (S2013 and Capan) in direct coculture with mouse neutrophils. Experimental conditions evaluated cancer cell only, cancer cell + neutrophil, cancer+neutrophil+GSK484 inhibitor, and cancer+GSK484 all ran in triplicate. Percent reduction is the fold change in cell number due to neutrophil killing of cancer cells. Percent reduction with GSK484 is the change in inhibition of cell killing by prevention of histone citrullination and the inability to produce NETs.

Effect of Neutrophil NETs on Cancer Growth In-Vivo

Based on in-vitro coculture experiment results, subsequent studies looked to test whether neutrophil cell killing would have a similar impact on tumor cells in-vivo. First, Miapaca-2 cells were altered by viral infection to express luciferase (Miapaca-2 -luc), and luminescence measured to verify luciferase expression. A growth curve comparing MiaPaca-2 and MiaPaca-2(luc) cells was performed and trypan blue exclusion assay verified that no significant differences in cellular growth was apparent between the two cell lines due to luciferase expression (Fig 12). MiaPaca-2-luc cells were injected intraperitoneally into mice and two days prior to termination of the experiment, mice were anesthetized and ultrasound performed to measure change in tumor volume (Fig13 B,C). It was observed that neutrophil depleted mice given administration of anti-Ly6G antibody had higher bioluminescence readings compared to the isotype control (Fig 13A). This would suggest that depletion of neutrophils would inhibit cancer growth, contrary, to what was observed with in-vitro cocultures when comparing changes in tumor growth by inhibition of NET production. Tumor volume showed a statistically significant increase in neutrophil depleted mice, indicating that neutrophils do not play a role in reducing tumor burden and instead may contribute to tumor growth.

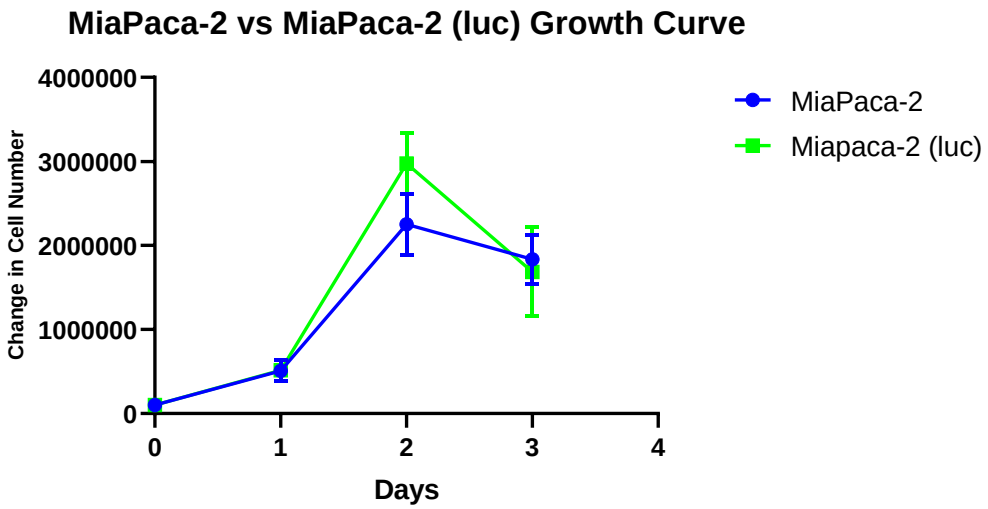

Figure 12. Growth curve comparing MiaPaca-2 with MiaPaca-2 luciferase expressing nonmetastatic cell lines. Cell counts correspond to time course of 24, 48, and 72 hours.

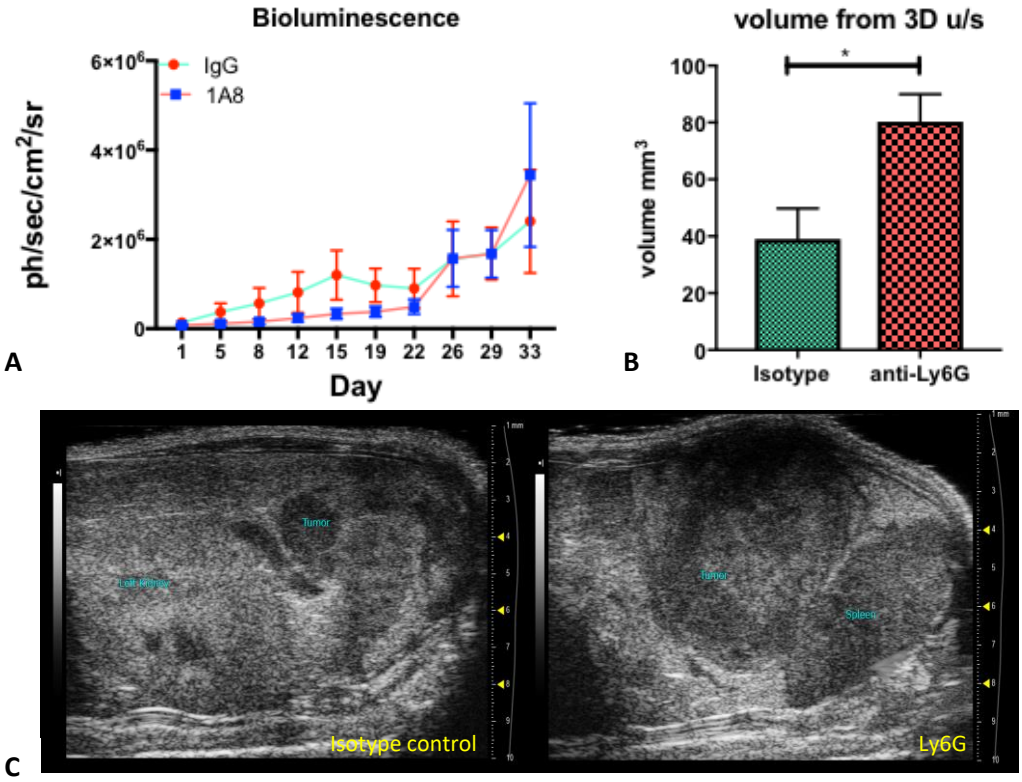

Fig 13. In vivo data from mouse study for injection of the Miapaca-Luc cells. (A) Bioluminescence reading of Miapaca luciferase expressing cells. Over course of 33 days anti-Ly6G(1A8) neutrophil depleted mice showed increase in cancer growth. (B) Ultrasound quantification of tumor volume changes in isotype control versus increased change in neutrophil depleted anti-Ly6G mice. (C) Representative ultrasound imaging of isotype control and Ly6G neutrophil depleted mice groups.

Chapter 4: Discussion

Through the preliminary experiments and those performed to validate initial findings, results were variable and at times contradict the original hypothesis of this study. Comparison of neutrophil survival in Miapaca-2 with Capan-1 conditioned medias on mouse derived neutrophils displayed higher number and viability at the 24hr time point. This could be indicative of a subpopulation of neutrophils present such as immature neutrophils after the 18hr time point. This is plausible as the isolation process for mice bone marrow derived neutrophils utilizing density centrifugation could have contained these immature cells. When compared to the human peripheral blood neutrophils a similar trend was observed with more neutrophils present at the 24 hours across all conditions (Fig 8B), when comparing metastatic and nonmetastatic cell lines. However, the two cell lines S2013 and CaPan-1 had lower number of neutrophils than S2007 (lung). This observation could indicate that as cancers progress further along the metastatic phenotype, they utilize neutrophils and their proteases by releasing soluble factors like granulocyte-macrophage colony-stimulating factor (GM-CSF) and extend neutrophil survival time (Garnot, 2015). However, further exploration into the composition of chemokines and soluble factors released by each metastatic cell line and their interaction with neutrophils is needed to better understand differences in survival advantages provided by metastatic and nonmetastatic cell types.

Mouse Sytox experiments comparing nonmetastatic (MiaPaca-2, AsPC1) and metastatic (Capan-1, S2013) conditioned medias on neutrophil NET formation showed differences with nonmetastatic conditioned medias having increased netosis. Although, these observations were not significant across cell line conditions. Conversely, when comparing the human blood derived neutrophils in these same conditions, significant differences were apparent in which nonmetastatic conditions induced NETosis in higher number of neutrophils as evidenced by increased neutrophil:NET ratios. Inherent differences in the functionality of neutrophils due to

species differences may be apparent when exposed to soluble factors produced by experimental conditioned medias. For example, neutrophils represent a smaller percentage of WBCs in mice (10-30%), whereas in humans, neutrophils are the predominant subpopulation of WBCs (Singhal, 2017). This information when combined with species differences in immunological defense strategies in which mice display more immune tolerance mechanisms developed to maintain low host risk at the expense of higher pathogen number, whereas humans predominately have immune resistant response directed to deactivate and rapidly eliminate pathogens, could explain how neutrophils when exposed to similar experimental conditions, could display such dissimilar responses (Eruslanov, 2017).

The characterization and visualization of neutrophils in patient tumor tissues has been one of the few reliable detections methods that correlates neutrophil counts with patient prognosis. With this understanding, our studies utilizing immunofluorescence antibodies for MPO and CitH3 showed no significant difference in NETs across pancreas, liver, and lung patient samples. However, a limitation of this study was low sample number of only six patients to examine. Concurrently, an additional limitation in this analysis is that neutrophil phenotypes and their activation states are difficult to quantify as their distribution and tumor heterogeneity can impact interpretation as to whether high neutrophil infiltration and netosis across samples were resultant of anti and pro-tumoral behavior. Moreover, though samples such as pancreas and lung display high accumulation of neutrophils and NETs, the different subset of neutrophils present in the tumor may be carrying different functions (Saha, 2016). Additionally, the absence or presence of chemotherapeutic drug regimens by each of the six patients could have altered cancer cell behavior and resultant cancer-neutrophil crosstalk as well as other cells within the microenvironment. For instance, significant changes in colocalization of MPO+CitH3 between chemotherapy treated versus non-treated groups was difficult to quantify as only one group of patient samples out of the six patients in total was untreated. Therefore, additional experiments

where greater number of both untreated and treated patient samples can be compared, could shed light on potential differences in neutrophil infiltration and activation in primary and metastatic tumor sites.

Cocultures of cancer cells with neutrophils in the absence and presence of GSK484 inhibition supported initial results that indicated inhibition of netosis would rescue cancer cell killing. This was most apparent in the nonmetastatic (MiaPaca-2, AsPC1) than in metastatic cell lines (Capan-1, S2013). Since metastatic cell numbers were also reduced in neutrophil containing cocultures, it would appear as if neutrophils are exhibiting anti-metastatic behavior. In the case of tumor progression, however, these observations may also be indicative of a supportive function of neutrophils in metastasis (Coffelt, 2016). In circulation, neutrophil activation by metastatic cells, results in endothelial and epithelial tissue damage mediated by NE and MMP9 which facilitates infiltration and migration of cancer cells to establish metastatic niche at more distant sites. Thus, our observations in these studies must be understood in the context that neutrophil-cancer cell interactions are incomplete without considering the tumor microenvironment and additional cell populations that play an integral part in neutrophil-cancer behavior when over a longer time span.

In relation to the impact of neutrophil NETs on cancer growth in-vivo, we found that depletion of neutrophils greatly attenuated the number of primary tumor cells in the peritoneal cavity, suggesting that neutrophils play an important role in primary tumor proliferation. This quantification was performed by measuring bioluminescence signals which provide insights as to the abundance and distribution of MiaPaca-2(luc) cells in mice. Notably, ultrasound images and tumor volume quantifications show significant increases in tumor size. However, when comparing this to the bioluminescence data (Fig 6A), it could be suggested that neutrophils may not be the only cell populations that aided in promoting tumor growth. In the first 15 days there was an initial lag in tumor size in the Ly6G depleted group when compared to control. However, from days 15-22, the control group showed a decrease in tumor cell proliferation while anti-Ly6G

group displayed minimal increases size. A potential explanation could be due to compensatory macrophage recruitment by cancer MiaPaca-2 (luc) cells. This has been observed in mouse tumor models targeting the inhibition of macrophages, with compensatory increases seen in tumor associated neutrophil infiltration at tumor sites (Nywening, 2018). For the control group, the initial increase in tumor size seen within the first two weeks could have elicited a slow antitumor macrophage response, but once macrophages remained in contact with the tumor cells over a period of 7 days, a transformation from antitumor to protumor phenotype may have occurred (Nywening, 2018). If this were the case, it could explain the subsequent increases in both the control and neutrophil depleted groups over the final 11 days of the study. This may be plausible as the Ly6G depleted groups' higher rate of growth may have been mediated through tumor associated macrophages, myeloid derived suppressor cells, as no neutrophil would be present in order to induce a protumor response. Alternatively, neutrophils may have the opposite effect as that seen in the in-vitro experiments. Instead, neutrophils could promote cancer growth, but when depleted would result in the initial lag seen in the first 2-3 weeks of the study in the anti-Ly6G group. Supporting evidence for this is seen in studies which showed that neutrophil derived NE was localized to endosomes and potentiated inositolposphatidyl-3 kinase (IP3) pathway mediated lung cancer cell proliferation (Houghton, 2010).

As it has been shown, neutrophils play a multifaceted role in cancer progression, proliferation, and metastasis. As illustrated in the experiments in this study, both anti-tumor and pro-tumoral roles have been postulated based on the data presented. Ultimately results of these studies highlight the possibility of tumor specific soluble factors mediating increases in neutrophil survival. In conjunction, neutrophil-cancer cell interactions and NETosis driven mechanisms affect neutrophil infiltration and NET formation in patient samples at primary and metastatic tissues sites. Notably, NET inhibition alleviates neutrophil antitumor responses in-vitro. However, opposing results of in-vivo experiments suggest neutrophils may be aiding tumor

proliferation by action of NETs and NET components such as NE and MMPs which are proinflammatory mediators pivotal in forming pro-tumorigenic environment which cancer cells utilize to grow, evolve, and metastasize to distant sites. Evident in this study is that mouse models allow for better understanding concepts of tumor biology, and microenvironment interactions. However, fundamental species differences in tumor heterogeneity and physiological interactions of neutrophil populations with cancer cells can impact their function as illustrated in the experiments discussed. These inherent differences pose challenges in translating data from mice studies to humans. Despite such hindrances, there is a continued need to develop and optimize novel approaches to studying this cell population in animal models and identify correlates to behavior and function in human cancer microenvironments.

Bibliograhy

1. Albrengues, J., Shields, M. A., Ng, D., Park, C. G., Ambrico, A., Poindexter, M. E., … Egeblad, M. (2018). Neutrophil extracellular traps produced during inflammation awaken dormant cancer cells in mice. *Science*. https://doi.org/10.1126/science.aao4227

2. Almyroudis NG, Grimm MJ, Davidson BA, Röhm M, Urban CF, Segal BH. NETosis and NADPH oxidase: At the intersection of host defense, inflammation, and injury. *Front Immunol*. 2013;4(MAR):1-7. doi:10.3389/fimmu.2013.00045

3. Amarsaikhan N, Elsawa A Misurelli SF, Neil MS, et al. GLI2 CD40 Ligand by the Transcription Factor Novel Molecular Mechanism of Regulation of. *J Immunol Ref*. 2017;198:4481-4489. doi:10.4049/jimmunol.1601490

4. Bekaii-Saab T, El-Rayes B. Current and emerging therapies in pancreatic cancer. *Curr Emerg Ther Pancreat Cancer*. 2017;23(7):1-379. doi:10.1007/978-3-319-58256-6

5. Biron BM, Chung C-S, O'brien XM, Chen Y, Reichner JS, Ayala A. Cl-amidine Prevents Histone 3 Citrullination, NET Formation, and Improves Survival in a Murine Sepsis Model. doi:10.1159/000448808

6. Boysen SR, Keir I, Letendre J-A, Li RHL, Tablin F. Article 291 Citation: Li RHL and Tablin F (2018) A Comparative Review of Neutrophil Extracellular Traps in Sepsis. *Front Vet Sci*. 2018;5:291. doi:10.3389/fvets.2018.00291

7. Campbell PJ, Yachida S, Mudie LJ, et al. pancreatic cancer. 2011;467(7319):1109-1113. doi:10.1038/nature09460.The

8. Carestia A, Kaufman T, Schattner M. Platelets: New bricks in the building of neutrophil extracellular traps. *Front Immunol*. 2016;7(JUL). doi:10.3389/fimmu.2016.00271

9. Cerutti C, Ridley AJ. Endothelial cell-cell adhesion and signaling. *Exp Cell Res*.

2017;358(1):31-38. doi:10.1016/j.yexcr.2017.06.003

10. Cheng H, Fan K, Luo G, Fan Z, Yang C, Huang Q. Kras G12D mutation contributes to regulatory T cell conversion through activation of the MEK / ERK pathway in pancreatic cancer. *Cancer Lett*. 2019;446(October 2018):103-111. doi:10.1016/j.canlet.2019.01.013

11. Chiorean EG. Pancreatic cancer : optimizing treatment options , new , and emerging targeted therapies. 2015:3529-3545.

12. Coffelt SB, Wellenstein MD, de Visser KE. Neutrophils in cancer: neutral no more. *Nat Publ Gr*. 2016;16. doi:10.1038/nrc.2016.52

13. Deryugina, E. I., & Quigley, J. P. (2015). Tumor angiogenesis: MMP-mediated induction of intravasation- and metastasis-sustaining neovasculature. *Matrix Biology*. https://doi.org/10.1016/j.matbio.2015.04.004

14. Distler M, Aust D, Weitz J, Pilarsky C, Grützmann R. Precursor lesions for sporadic pancreatic cancer: PanIN, IPMN, and MCN. *Biomed Res Int*. 2014;2014:474905. doi:10.1155/2014/474905

15. Erkan M, Michalski CW, Rieder S, et al. The Activated Stroma Index Is a Novel and Independent Prognostic Marker in Pancreatic Ductal Adenocarcinoma. *Clin Gastroenterol Hepatol*. 2008;6(10):1155-1161. doi:10.1016/j.cgh.2008.05.006

16. Eruslanov EB, Singhal S, Albelda SM. Mouse versus Human Neutrophils in Cancer: A Major Knowledge Gap. *Trends in Cancer*. 2017;3(2):149-160. doi:10.1016/j.trecan.2016.12.006

17. Felix K, Gaida MM. Neutrophil-Derived Proteases in the Microenvironment of Pancreatic Cancer -Active Players in Tumor Progression. *Int J Biol Sci*. 2016;12(3):302-313. doi:10.7150/ijbs.14996

18. Feng, M., Xiong, G., Cao, Z., Yang, G., Zheng, S., Song, X., … Zhao, Y. (2017). PD-1/PD-L1 and immunotherapy for pancreatic cancer. *Cancer Letters*, *407*, 57–65. https://doi.org/10.1016/j.canlet.2017.08.006

19. Fridlender ZG, Sun J, Kim S, et al. Polarization of Tumor-Associated Neutrophil Phenotype by TGF-β: "N1" versus "N2" TAN. *Cancer Cell*. 2009;16(3):183-194. doi:10.1016/j.ccr.2009.06.017

20. Gabrilovich, D. I., Ostrand-Rosenberg, S., & Bronte, V. (2012). Coordinated regulation of myeloid cells by tumours. *Nature Reviews Immunology*. https://doi.org/10.1038/nri3175

21. Granot Z, Jablonska J. Distinct Functions of Neutrophil in Cancer and Its Regulation. *Mediators Inflamm*. 2015;2015:701067. doi:10.1155/2015/701067

22. Guo J, Xie K, Zheng S. Molecular Biomarkers of Pancreatic Intraepithelial Neoplasia and Their Implications in Early Diagnosis and Therapeutic Intervention of Pancreatic Cancer. *Int J Biol Sci*. 2016;12(3):292-301. doi:10.7150/ijbs.14995

23. Ilic M, Ilic I. Epidemiology of pancreatic cancer. 2016;22(44):9694-9705. doi:10.3748/wjg.v22.i44.9694

24. Jurasz P, Alonso-Escolano D, Radomski MW. Platelet--cancer interactions: mechanisms and pharmacology of tumour cell-induced platelet aggregation. *Br J Pharmacol*. 2004;143(7):819-826. doi:10.1038/sj.bjp.0706013

25. Knight JS, Zhao W, Luo W, Subramanian V, O'dell AA, Yalavarthi S, et al. Peptidylarginine deiminase inhibition is immunomodulatory and vasculoprotective in murine lupus. J Clin Invest. (2013) 123:2981–93. doi: 10.1172/JCI67390

26. Koikawa K, Ohuchida K, Ando Y, et al. Basement membrane destruction by pancreatic stellate cells leads to local invasion in pancreatic ductal adenocarcinoma. *Cancer Lett*.

2018;425:65-77. doi:10.1016/j.canlet.2018.03.031

27. Kruger P, Saffarzadeh M, Weber ANR, et al. Neutrophils : Between Host Defence , Immune Modulation , and Tissue Injury. 2015;(i):1-23. doi:10.1371/journal.ppat.1004651

28. Lewis HD, Liddle J, Coote JE, et al. HHS Public Access. *Nat Chem Biol*. 2015;11(3):189-191. doi:10.1038/nchembio.1735.Inhibition

29. Makohon-moore A, Iacobuzio-donahue CA. Pancreatic cancer biology and genetics from an evolutionary perspective. *Nat Publ Gr*. 2016;16(9):553-565. doi:10.1038/nrc.2016.66

30. Mantoni TS, Lunardi S, Al-Assar O, Masamune A, Brunner TB. Pancreatic stellate cells radioprotect pancreatic cancer cells through β1-integrin signaling. *Cancer Res*. 2011;71(10):3453-3458. doi:10.1158/0008-5472.CAN-10-1633

31. Marvel D, Gabrilovich DI. Myeloid-derived suppressor cells in the tumor microenvironment : expect the unexpected. 2015;125(9). doi:10.1172/JCI80005.Definition

32. Matrisian LM, Berlin JD. Trials. 2019:205-215.

33. Maugeri N, Campana L, Gavina M, et al. Activated platelets present high mobility group box 1 to neutrophils, inducing autophagy and promoting the extrusion of neutrophil extracellular traps. *J Thromb Haemost*. 2014;12(12):2074-2088. doi:10.1111/jth.12710

34. McCarroll JA, Naim S, Sharbeen G, et al. Role of pancreatic stellate cells in chemoresistance in pancreatic cancer. *Front Physiol*. 2014;5:141. doi:10.3389/fphys.2014.00141

35. Meri RR, Puolakkainen PA. ScienceDirect Tumor-associated macrophages (TAMs) as biomarkers for gastric cancer : A review. 2018;4:156-163. doi:10.1016/j.cdtm.2018.07.001

36. Merza M, Hartman H, Rahman M, et al. Neutrophil Extracellular Traps Induce Trypsin

Activation, Inflammation, and Tissue Damage in Mice With Severe Acute Pancreatitis. 2015. doi:10.1053/j.gastro.2015.08.026

37. Miksch RC, Schoenberg MB, Weniger M, et al. Prognostic Impact of Tumor-Infiltrating Lymphocytes and Neutrophils on Survival of Patients with Upfront Resection of Pancreatic Cancer. *Cancers (Basel)*. 2019;11(1). doi:10.3390/cancers11010039

38. Miyata, T., & Fan, X. (2012). A second hit for TMA. *Blood*, 120(6), 1152-1154.Accessed April 25, 2019. https://doi.org/10.1182/blood-2012-06-433235.

39. Morrison AH, Byrne KT, Vonderheide RH. Immunotherapy and Prevention of Pancreatic Cancer. *Trends in Cancer*. 2018;4(6):418-428. doi:10.1016/j.trecan.2018.04.001

40. Nicolás-Ávila, J. Á., Adrover, J. M., & Hidalgo, A. (2017). Neutrophils in Homeostasis, Immunity, and Cancer. *Immunity*, *46*(1), 15–28. https://doi.org/10.1016/j.immuni.2016.12.012

41. Nywening TM, Belt BA, Cullinan DR, et al. Targeting both tumour-associated CXCR2+ neutrophils and CCR2+ macrophages disrupts myeloid recruitment and improves chemotherapeutic responses in pancreatic ductal adenocarcinoma. *Gut*. 2018;67(6):1112-1123. doi:10.1136/gutjnl-2017-313738

42. Olsson AK, Cedervall J. The pro-inflammatory role of platelets in cancer. *Platelets*. 2018;29(6):569-573. doi:10.1080/09537104.2018.1453059

43. Petrushnko W, Gundara JS, De Reuver PR, O'grady G, Samra JS, Mittal A. Systematic review of peri-operative prognostic biomarkers in pancreatic ductal adenocarcinoma. 2016. doi:10.1016/j.hpb.2016.05.004

44. Piccard H, Muschel RJ, Opdenakker G: On the dual roles and polarized phenotypes of neutrophils in tumor development and progression. *Crit Rev Oncol Hematol* 2012, 82:296-309

45. Pittman ME, Rao R, Hruban RH. Classification, Morphology, Molecular Pathogenesis, and Outcome of Premalignant Lesions of the Pancreas. *Arch Pathol Lab Med*. 2017;141:1606-1614. doi:10.5858/arpa.2016-0426-RA

46. Polireddy K, Chen Q. Cancer of the pancreas: Molecular pathways and current advancement in treatment. *J Cancer*. 2016;7(11):1497-1514. doi:10.7150/jca.14922

47. Porembka, M. R., Mitchem, J. B., Belt, B. A., Hsieh, C. S., Lee, H. M., Herndon, J., … Goedegebuure, P. (2012). Pancreatic adenocarcinoma induces bone marrow mobilization of myeloid-derived suppressor cells which promote primary tumor growth. *Cancer Immunology, Immunotherapy*. https://doi.org/10.1007/s00262-011-1178-0

48. Puleo, F.; Nicolle, R.; Blum, Y.; Cros, J.; Marisa, L.; Demetter, P.; Quertinmont, E.; Svrcek, M.; Elarouci, N.; Iovanna, J.; et al. Stratification of pancreatic ductal adenocarcinomas based on tumor and microenvironment features. Gastroenterology 2018, 155, 1999.e3–2013.e3.

49. Reid MD, Basturk O, Thirabanjasak D, et al. Tumor-infiltrating neutrophils in pancreatic neoplasia. *Mod Pathol*. 2011;24(12):1612-1619. doi:10.1038/modpathol.2011.113

50. Rohrbach AS, Slade DJ, Thompson PR, Mowen KA. Activation of PAD4 in NET formation. *Front Immunol*. 2012;3(NOV). doi:10.3389/fimmu.2012.00360

51. Saffarzadeh M. Neutrophil Extracellular Traps as a Drug Target to Counteract Chronic and Acute Inflammation. *Curr Pharm Biotechnol*. 2019;20(January). doi:10.2174/1389201020666190111164145

52. Saha S, Biswas SK. Tumor-Associated Neutrophils Show Phenotypic and Functional Divergence in Human Lung Cancer. 2016. doi:10.1016/j.ccell.2016.06.0161.

53. Sohal DPS, Willingham FF, Falconi M, Raphael KL, Crippa S. Pancreatic Adenocarcinoma: Improving Prevention and Survivorship. *Am Soc Clin Oncol Educ B*. 2017;37:301-310. doi:10.14694/EDBK_175222

54. Stromnes IM, Brockenbrough JS, Izeradjene K, et al. Targeted depletion of an MDSC subset unmasks pancreatic ductal adenocarcinoma to adaptive immunity. *Gut*. 2014;63(11):1769-1781. doi:10.1136/gutjnl-2013-306271

55. Torphy RJ, Zhu Y, Schulick RD. Immunotherapy for pancreatic cancer: Barriers and breakthroughs. *Ann Gastroenterol Surg*. 2018;2(4):274-281. doi:10.1002/ags3.12176

56. Vonderheide RH, Bajor DL, Winograd R, Evans RA, Bayne LJ, Beatty GL. CD40 immunotherapy for pancreatic cancer. *Cancer Immunol Immunother*. 2013;62(5):949-954. doi:10.1007/s00262-013-1427-5

57. Wang-Gillam, A., Li, C. P., Bodoky, G., Dean, A., Shan, Y. S., Jameson, G., … Chen, L. T. (2016). Nanoliposomal irinotecan with fluorouracil and folinic acid in metastatic pancreatic cancer after previous gemcitabine-based therapy (NAPOLI-1): A global, randomised, open-label, phase 3 trial. *The Lancet*. https://doi.org/10.1016/S0140-6736(15)00986-1

58. Wang X, Khalil RA. HHS Public Access. 2019;(617):1-73. doi:10.1016/bs.apha.2017.08.002.Matrix

59. Wargo, J. A., Reddy, S. M., Reuben, A., & Sharma, P. (2016). Monitoring immune responses in the tumor microenvironment. *Current Opinion in Immunology*. https://doi.org/10.1016/j.coi.2016.05.006